

Old Dominion University

ODU Digital Commons

Civil & Environmental Engineering Master's
Projects

Civil & Environmental Engineering

2018

Investigation of Ribbed Dome including Tuned Mass Damper

Ali Parva

Old Dominion University, ali.parva1@gmail.com

Follow this and additional works at: https://digitalcommons.odu.edu/cee_me_projects



Part of the [Civil Engineering Commons](#), and the [Structural Engineering Commons](#)

Recommended Citation

Parva, Ali, "Investigation of Ribbed Dome including Tuned Mass Damper" (2018). *Civil & Environmental Engineering Master's Projects*. 1.

https://digitalcommons.odu.edu/cee_me_projects/1

This Master's Project is brought to you for free and open access by the Civil & Environmental Engineering at ODU Digital Commons. It has been accepted for inclusion in Civil & Environmental Engineering Master's Projects by an authorized administrator of ODU Digital Commons. For more information, please contact digitalcommons@odu.edu.

Investigation of Ribbed Dome including Tuned Mass Damper

Structure research report

By
Ali Parva

Supervisor: Dr. Zia Razzaq
Dr. Mojtaba Sirjani
Dr. Shahin Nayyeri Amiri



Department of Civil and Environmental Engineering

Old Dominion University

Norfolk VA 23529

December 2019

Investigation of Ribbed Dome including Tuned Mass Damper

by

Ali Parva

B.S. September 2012, Shiraz Azad University
M.A. September 2015, Shahid Beheshti University

A Project Submitted to the Faculty of
Old Dominion University in Partial Fulfillment of the
Requirements for the Degree of

MASTER OF ENGINEERING

CIVIL & ENVIRONMENTAL ENGINEERING

OLD DOMINION UNIVERSITY
December 2018

Approved by:

Dr. Zia Razzaq (Director)

Dr. Mojtaba Sirjani (Member)

Dr. Shahin Nayyeri Amiri (Member)

ABSTRACT

INVESTIGATION OF RIBBED DOME INCLUDIG TUNED MASS DAMPER

Ali Parva
Old Dominion University, 2018
Director: Dr. Zia Razzaq

This research report presents the outcome of an investigation of lightweight ribbed steel dome structure. The proposed ribbed dome structure is studied both numerically and experimentally under static, natural vibration, and base excitation conditions. The base excitation is considered in the form of a sinusoidal as well as seismic loading in the form of a scaled-down 1940 El Centro earthquake. A numerical study of the ribbed dome is also conducted including a tuned mass damper (TMD). The performance of the dome is also compared with that of a hexagonal vertical structure showing a superior response of the dome under seismic loading. Both experimental and theoretical results with TMD are in good agreement. Lastly, the numerical study shows a significant decrease in vibration of the ribbed dome when TMD is utilized.

Copyright, 2018, by Ali Parva, All Rights Reserved.

ACKNOWLEDGMENT

I would like to express my special appreciation and thanks to my advisor Professor Dr. Zia Razzaq, you have been a tremendous mentor for me. Your advice on both research as well as on my career have been invaluable. I would also like to thank my committee members, Professor Sirjani and Professor Nayyeri Amiri, for generously offering their time, support, guidance and good will throughout the preparation and review of this document.

A special thanks to my family. Words cannot express how grateful I am to my mother, brother, sister, brother in law, Moones, Arshan, and my cousin, for all of the sacrifices that you've made on my behalf. Thank you for supporting me for everything, and especially I can't thank you enough for encouraging me throughout this experience.

My thanks and appreciations also go to my colleagues, Ramin Rabiee who willingly helped me out with his abilities, Farid Tavakol, Elham Sharifi and Maryam Ehsaei in developing the project.

NOMENCLATURE

| | |
|--------------|-------------------------|
| C | Structure Global Matrix |
| C_d | Damping of Damper |
| K | Global Stiffness |
| K_d | Stiffness of Damper |
| M | Mass Matrix |
| M_d | Mass of Damper |
| R | External Force |
| U | Displacement |
| \dot{U} | Velocity |
| \dot{U}_d | Velocity of Damper |
| \ddot{U} | Acceleration |
| \ddot{U}_d | Acceleration of Damper |
| ω | Natural Frequency |
| γ | Mass Ratio |
| ζ | Damping |

TABLE OF CONTENTS

| | |
|--|-------------------------------------|
| ABSTRACT..... | iii |
| ACKNOLEDGMENT | v |
| NOMENCLATURE..... | vi |
| LIST OF TABELS | viii |
| LIST OF FIGURES | ix |
| 1. INTRODUCTION..... | 1 |
| 1.1 Background..... | 1 |
| 1.2 Literature Review..... | 2 |
| 1.2.1 Dampers..... | 2 |
| 1.2.1.1 Active Control Devices | 2 |
| 1.2.1.2 Semi-Active Control Devices..... | 2 |
| 1.2.1.3 Hybrid Control Devices | 4 |
| 1.2.1.4 Passive Control Devices:..... | 5 |
| 1.2.4.1 Tuned Mass Damper and Practical Implementation..... | 5 |
| 1.2.2 Domes..... | 10 |
| 1.2.2.1 A Brief History of the Dome | 10 |
| 1.2.2.2 Dome Types | 12 |
| 1.3 Problem Statement..... | 13 |
| 1.4 Objective and Scope | 13 |
| 1.5 Assumptions and Conditions..... | 14 |
| 2. EXPERIMENTAL STUDY | 15 |
| 2.1 Test Specimens and Material Properties | 15 |
| 2.1.1 Beam Bending Test..... | Error! Bookmark not defined. |
| 2.2 Test Set-up and Procedure | 15 |
| 2.2.1 Static Test | 20 |
| 2.2.1.1 Load Deflection Test..... | Error! Bookmark not defined. |
| 2.2.2 Vibration Test | 22 |
| 2.2.2.1 Natural Vibration Test | 22 |
| 2.2.2.2 Base Excitation Test..... | 23 |

| | |
|--|-------------------------------------|
| 3. THEORETICAL STUDY | 32 |
| 3.1 Methodology | 32 |
| 3.2 Numerical Modeling..... | 34 |
| 3.2.1 SAP Modeling..... | 34 |
| 3.2.1 Static Test | 35 |
| 3.2.1.1 Load Deflection Test..... | Error! Bookmark not defined. |
| 3.2.2 Vibration Test | 37 |
| 3.2.2.1 Natural Vibration test..... | 37 |
| 3.2.2.1 Geometry Effectiveness Test..... | 39 |
| 3.2.2.2 Base Excitation Test with TMD..... | 41 |
| 4. ARCHITECTURAL DESIGN..... | 47 |
| 4.1 Proposed Architectural Design | 47 |
| 4.1.1 Affordable Housing | 49 |
| 4.1.2 Advantages of the Design | 50 |
| 4.1.3 How to Build a Residential Dome | 51 |
| 5. CUNCLUSION AND FUTURE RESEARCH..... | 55 |
| 5.1 Conclusion..... | 55 |
| 5.2 Future scope for study: | 56 |
| References | 57 |

LIST OF TABELS

| | |
|--|-------------------------------------|
| Table 1: load deflection relation of the dome material..... | Error! Bookmark not defined. |
| Table 2: Dome elements specifications..... | Error! Bookmark not defined. |
| Table 3: Exp. load deflection test results | 21 |
| Table 3: Exp. And Num. load deflection tests results..... | Error! Bookmark not defined. |

| | |
|---|-----------|
| Table 4: Logarithmic Increment results of Exp. and Num. | 38 |
|---|-----------|

LIST OF FIGURES

| | |
|--|-------------------------------------|
| Figure 1: Kyobashi Seiwa Building [15] | 3 |
| Figure 2: Dongting Lake Bridge in Hunan, China [15]..... | 3 |
| Figure 3: Sendagaya INTES building in Tokyo [15] | 4 |
| Figure 4: Parliaments Building (Left), Figure 5: US Court of Appeals (Right) | 5 |
| Figure 6: Centre Tower,Sydney, Figure 7: Citicrop Centre, NYC | 7 |
| Figure 8: Burj Al Arab, Dubai..... | 8 |
| Figure 9: Taipai 101..... | 9 |
| Figure 10: Spire of Dublin..... | 9 |
| Figure 11: Zulu Hut (KwaZulu-Natal) | 10 |
| Figure 12: Musgum Farmstead (Kirchner [9]) | 11 |
| Figure 13: The Ramesseum Storage Vaults, Gourn, Egypt..... | 11 |
| Figure 14: Common Dome Types Geometry – Buckminster Fuller¹⁹ institute [17]..... | 12 |
| Figure 15: Isometric view of the Ribbed Dome Structure | 13 |
| Figure 16: Structure material Load-Deflection relation | Error! Bookmark not defined. |
| Figure 17: Isometric view of the dome..... | Error! Bookmark not defined. |
| Figure 18: Isometric view of the dome and the base supports locations..... | 15 |
| Figure 19: Isometric view of accelerometers locations | 16 |
| Figure 20: Structure Elements order of labeling | 17 |
| Figure 21: Dome ring’s plan view..... | 19 |
| Figure 22: Structure load-deflection test set up. | 20 |

| | |
|---|-------------------------------------|
| Figure 23: Experimental acceleration vs. time relation | 22 |
| Figure 24: Experimental acceleration vs. time relation (Call Out) | Error! Bookmark not defined. |
| Figure 25: Accelerometers Locations on the dome structure | 24 |
| Figure 26: Exp. Acceleration vs. time relation of Node 1 in sinusoidal base excitation | 25 |
| Figure 27: Exp. Acceleration vs. time relation of Node 2 in sinusoidal base excitation | 25 |
| Figure 28: Exp. Acceleration vs. time relation of Node 3 in sinusoidal base excitation | 26 |
| Figure 29: Exp. Acceleration vs. time relation of Node 4 in sinusoidal base excitation | 26 |
| Figure 30: Experimental acceleration vs. time relation comparison | Error! Bookmark not defined. |
| Figure 31: Experimental El Centro earthquake Response | 28 |
| Figure 32: Unidirectional Forcing function vs. time relation of the EL Centro Earthqk.... | 29 |
| Figure 33: Displacement vs. time relation of the EL Centro Earthquake..... | 29 |
| Figure 34: Acceleration vs. time relation of the EL Centro Earthquake | 30 |
| Figure 35: Unidirectional Forcing function vs. time relation of the sinusoidal vibration.... | 30 |
| Figure 36: Displacement vs. time relation of the sinusoidal vibration..... | 31 |
| Figure 37: Acceleration vs. time relation of the sinusoidal vibration | 31 |
| Figure 38: Isometric view of SAP2000 model..... | 35 |
| Figure 39: Load-Deflection of the SAP model..... | Error! Bookmark not defined. |
| Figure 40: load-deflection relationship of both experimental and numerical..... | 36 |
| Figure 41: Acceleration vs. time relation of the Numerical free vibration..... | 37 |
| Figure 42: Acceleration vs. time relation of both exp. And Num. free vibration..... | Error! Bookmark not defined. |

| | |
|---|-----------|
| Figure 43: Acceleration vs. time relation of both exp. And Num. free vibration (Call out) | 37 |
| Figure 44: Acceleration versus time relation of the dome numerical model..... | 38 |
| Figure 45: Acceleration versus time relation of numerical study of hexagonal structure ... | 39 |
| Figure 46: Acceleration versus time relation of the dome numerical model..... | 40 |
| Figure 47: Numerical result of Acceleration versus time relation of the dome and hexagonal | 40 |
| Figure 48: Isometric view of hexagonal SAP model | 41 |
| Figure 49: TMD Mass Ratio increment in numerical model..... | 42 |
| Figure 50: SAP model response of TMD | 43 |
| Figure 51: Mass Ratio versus max. Acceleration relation of the numerical dome model.... | 44 |
| Figure 52: Response of the numerical and experimental dome to the sinusoidal vibration | 44 |
| Figure 53: Response of the numerical and experimental dome to the El Centro vibration | 46 |
| Figure 54: Experiment Set up..... | 46 |
| Figure 55: Dome Types..... | 48 |
| Figure 56: Typical dome Construction Procedure | 52 |
| Figure 57: Proposed Architectural proposed design plan view..... | 52 |
| Figure 58: Architectural proposed design plan view..... | 53 |
| Figure 59: Architectural proposed design section View..... | 54 |

1. INTRODUCTION

1.1 Background

A vast number of human lives are lost or affected due to structures collapsing during earthquakes. One significant cause of such collapses is the rather heavy but weak structures and materials used in both residential and commercial buildings. Thus, the challenge of an evaluation of strong but light-weight structures subjected to earthquakes still remains. Presented in this research report is an experimental and numerical study of a light-weight and resilient ribbed dome structure for possible use as a dwelling. Although many types of dome structures such as geodesic, lamella, or monolithic dome already exist, there is a need for relatively strong, and inexpensive dome for single-family use which can readily be transported to any given seismically active regions.

In this research project both static and dynamic behavior of the ribbed dome structure is studied. Due to the geometry of domed structures, they tend to be more stable and resilient when subjected to dynamic and extreme loading conditions. Nevertheless there is still a need for absorbing the energy of vibration with the goal of minimizing or eliminating damage or collapse.

Results based on laboratory experiments conducted on a small-scale ribbed dome are presented under static loading, natural vibration, and base excitation in the absence of tuned mass damper. A comparable numerical study is also conducted using SAP2000 software. The performance of a tuned mass damper is investigated only theoretically using SAP2000.

1.2 Literature Review

A brief literature review related to some types and vibration dampers is presented in this section. Various types of vibration control techniques have been used in the past which can be broadly classified into four categories. Active control, Passive control, Semi-active control and, Hybrid control.

1.2.1 Dampers

A brief overview of vibration controlling techniques is presented herein.

1.2.1.1 Active Control Devices

Active Controlling devices use an external power source to control actuators to apply forces on the structures. Signals that are a function of responses of the structure are sent to the actuators. Equipment requirements are considered more in active control strategies than passive control, thereby increasing the cost and maintenance of such systems. Active tuned mass damper, active tuned liquid column damper and active variable stiffness damper are some of the examples of active control devices. An outstanding example for this technique is: Applications - AMD on Kyobashi Seiwa Building, Duox on ANDO Nighikicho, Trigon on Shinjuku Tower. Padmabati Sahoo [8].

1.2.1.2 Semi-Active Control Devices

Semi-active control devices utilize the external energy less than that of active devices. This approach unites the optimistic aspects of passive and active control devices. These devices generate forces as a result of the motion of the structure and cannot add energy to the structural system. Variable orifice dampers,

variable friction dampers, variable stiffness damper, and controllable fluid dampers are some of the examples of semi active control devices.

Outstanding examples for this technique are: Applications- Kajima Shizuoka Building in Shizuoka, Japan, Walnut Creek Bridge in Oklahoma, 11-storey building CEPCO Gifu Japan, Keio University School of Science and Technology Tokyo in Japan. Dongting Lake Bridge in Hunan, China.



Figure 1: Kyobashi Seiwa Building (Active control device) [15]



Figure 2: Dongting Lake Bridge in Hunan, China (semi active control device)[15]

1.2.1.3 Hybrid Control Devices

Hybrid Control devices combine the passive, active or semi-active devices to achieve higher level of performance. Since a portion of the control objective is accomplished by the passive system, less power resource is required. A side benefit of hybrid systems is that, in the case of a power failure, the passive components of the control still offer protection, unlike a fully active control system. Examples of hybrid control devices include hybrid mass damper and hybrid base isolation. Applications- Sendagaya INTES building in Tokyo. Padmabati Sahoo [8].



Figure 3: Sendagaya INTES building in Tokyo (Hybrid control device)[15]

1.2.1.4 Passive Control Devices:

Passive Control device impart forces that are developed in response to the motion of the structures. By absorbing some of the input energy, they reduce the energy dissipation demand on the structure. Therefore no external power source is required to add energy to the structural system. Base isolation, tuned mass dampers (TMD), tuned liquid dampers (TLD), metallic yield dampers, viscous fluid dampers are some of the examples of passive control devices.

Outstanding examples for this technique are: Applications - city halls of Oakland, US Court of Appeals in San Francisco (Friction Pendulum), NZ Parliament Building and the associated Assembly Library and the new Museum of NZ, Matsumura Research Institute building in Kobe. Padmabati Sahoo [8].



Figure 4: Parliaments Building **Figure 5:** US Court of Appeals (Passive control device)

1.2.4.1 Tuned Mass Damper and Practical Implementation

The concept of TMD was first used by Frahm in 1909 to diminish the undulating motion of ships as well as ship hull vibrations. Later, Hartog in 1940 developed analytical model for vibration controlling power of TMD. Then he optimized TMDs parameter for

sinusoidal excitations. Fahim considered different parameters like mass ratio, frequency ratio, damping ratio etc. to obtain the optimum parameters which are used to compute the response of various single degree of freedom and multi degree of freedom structures with TMD at different earthquake excitation. The optimum parameters obtained are helpful in reducing the displacement and acceleration response significantly. Sain [11]

Tuned mass damper is a passive control device connected to the structure like a secondary mass to reduce the dynamic response of the structure and increases the damping capacity. It has been widely used for vibration control in many mechanical engineering systems. Recently many related have been adopted to reduce vibration in civil engineering structures because of their easy and simple mechanism. To obtain optimum response the natural frequency of the secondary mass is always tuned to that of primary structure such that when that particular frequency of the structure get excited, the TMD will resonate out of phase with the structural motion. The excess amount of energy built up in the structure is transfered to the secondary mass and dissipated due to relative motion developed between them at a later stage. Till now many tuned mass dampers have been installed worldwide. Centre point Tower in Sydney, Australia is the first structure in which TMD was installed. TMD is also installed in two buildings in the United States. In one case, a 279 M high TMD is placed on the 63rd floor in topmost point of the structure, having a mass of 366 kN, with a linear damping of from 8-14%, reducing the amplitude of the building by 50%.



Figure 6: Centre Tower, Sydney (TMD)



Figure 7: Citicorp Centre, NYC (TMD)

Two dampers are installed in 60th floor of John Hancock Tower in Boston, to reduce structural vibration caused by wind, each having a 2700 kN weight with a lead filled steel box of 5.2 square meter and 1m deep sliding on a 9m long steel plate. Berlin TV tower, one of the tallest structures of Germany constructed between 1965 and 1969, in this 368 meters high building a tuned mass damper is installed. The entrance of observation deck is 6.25 m above ground with 2 tones lifts for transport of visitors. Weight of the sphere is 4800 tones and its diameter is 32 m. There is a steel stairway with 986 steps.

Burj Al Arab, a luxury hotel in Dubai, is the 3rd tallest hotel in the world with installed with 11 tuned mass dampers. 39% of the total height is made up of non-occupied space. Padmabati Sahoo [8].



Figure 8: Burj Al Arab, Dubai (Passive control device)

Perk Tower, Chicago, 257 m tall with 70 floors is the eleventh tallest building in Chicago, the 39th tallest building in the United States, and the eighty-third tallest in the world and the 1st structure in United States to be designed with a tuned mass damper to counteract the wind effect on the structure. It is a 300 ton massive steel pendulum damper hanging from 4 cables inside a cage which stabilizes the building from swaying in the wind.

Taipai 101, in Taiwan which was the world's tallest building from 2004 to 2010, consists of 101 above ground and 5 underground floors, is equipped with a steel pendulum that serves as a tuned mass damper suspended from the 92nd to the 87th floor. The pendulum sways to offset movements in the building caused by strong gusts. It is the largest damper sphere in the world, consists of 41 circular steel plates of varying diameters, each 125 mm thick, welded together to form a 5.5 m diameter sphere. Two additional tuned mass dampers, each weighing 6 tons (7 short tons), are installed at the tip of the spire which help prevent damage to the structure due to strong wind loads.



Figure 9: Taipei 101 (Passive control device)

Spire of Dublin (Monument of Light), 121.2 m in height is the largest stainless steel monument located in Dublin, Ireland. It has an elongated cone of diameter 3 m diameter at the base, narrowing to 515 cm at the top. It is constructed from eight hollow tubes of stainless steel and equipped with a tuned mass damper to counteract sway.



Figure 10: Spire of Dublin (Passive control device)

1.2.2 Domes

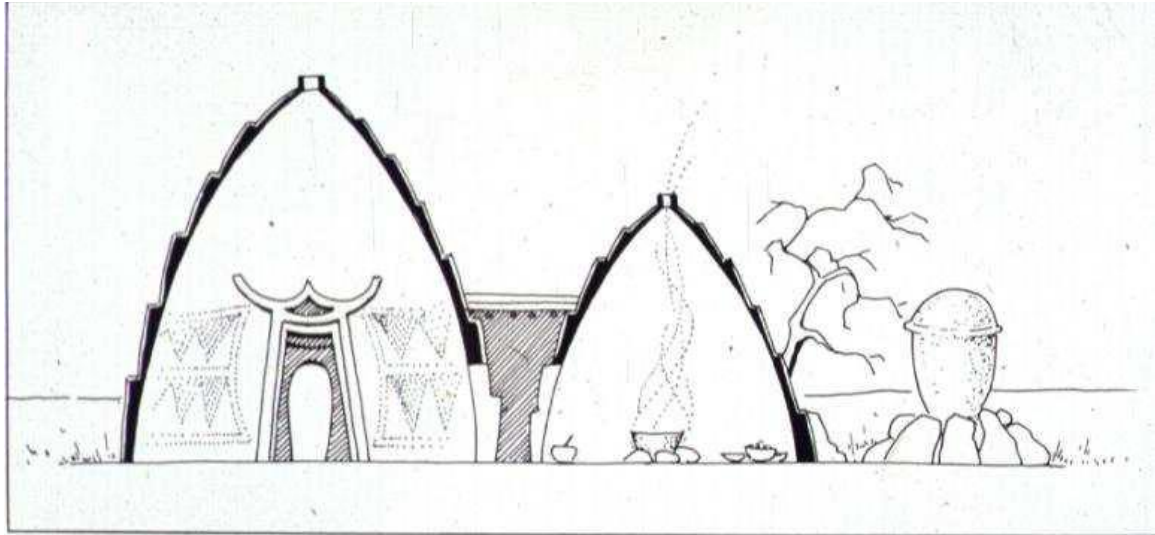
1.2.2.1 A Brief History of the Domes

Domes have been used throughout the ages as a housing form, or an element of a housing form (roof structure). African and aboriginal societies built domes by planting branches in the ground and weaving the dome shape, Kirchner [9]. Figure 11 shows a typical Zulu hut in Kwazulu-Natal, South Africa.



Figure 11: Zulu Hut (KwaZulu-Natal)

The dome was also used by the Musgum tribe of Cameroon. This parabolic dome consists of a highly cohesive earth shell, 15-20cm (5.9-7.9 inches) thick at its base, 5cm (1.97 inches) thick at the top and 7-8m (23-26 ft) high. Figure 12 shows a typical Musgum dome. Gardi [6]



Cross-section of a Musgum farmstead.

Figure 12: Musgum Farmstead, Kirchner [9]

The dome shape has also been used historically to span large distances. The Moguls, Egyptians, Byzantines and Romans used domes and vaults extensively. Examples of these are The Shrine of the Living King (Samarkand) built by the Moguls, The Pantheon in Rome and The Temple of Ramses II (near Aswan). The Temple of Ramses II was constructed out of bricks in 1290BC and parts of the structure, such as the vaults where the priests stored grain, are still standing. This illustrates the great potential of earth as a durable construction material. Kirchner [9].



Figure 13: The Ramesseum Storage Vaults, Gournah, Egypt

1.2.2.2 Dome Types

In general, domes are designed and built in different geometries. Each one of them has its own structural properties. Figure 14 presents the most common dome geometry in the design field.

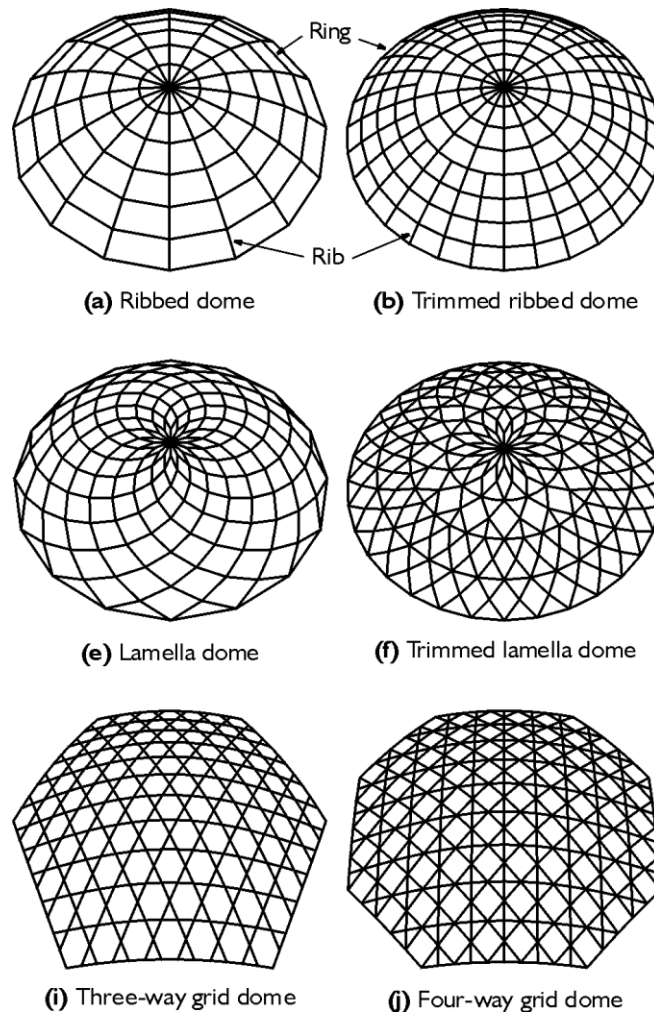


Figure 14: Common Dome Types Geometry, Buckminster Fuller¹⁹ institute [17]

General types of the dome are: Beehive dome, Braced dome, Cloister vault, Compound dome, Crossed-arch dome, Ellipsoidal dome, Geodesic dome, Hemispherical dome, Onion

dome, Oval dome, Paraboloid dome, Sail dome, Saucer dome, Umbrella dome. Wikipedia [19]

1.3 Problem Statement

Figure 15 shows a scaled-down model of a ribbed steel dome structure studied in this research project. It is subjected to a static load, natural vibration, and base excitation, respectively. The problem addressed here is that of determining the effectiveness of tuned mass damper under both sinusoidal vibrations as well as scaled-down El Centro earthquake of 1940. In addition to the TMD effectiveness, the application of the dome geometry in reducing the response of the system is studied. A feasible tentative architectural plan for an economical structure dwelling is also considered.

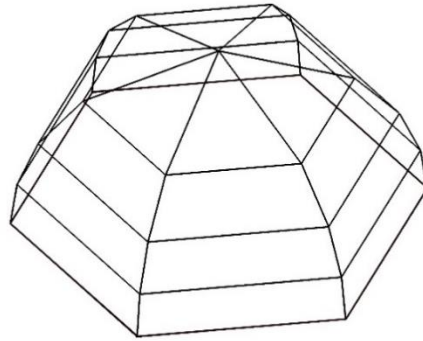


Figure 15: Isometric view of the Ribbed Dome Structure

1.4 Objectives and Scope

The objective of the present work is to conduct an analysis and series of laboratory experiments to study the seismic behavior of ribbed dome structure. Furthermore, the design aims at the numerical study of demonstrating the seismic performance improvements when the tuned mass damper (TMD) utilized. The study represents the effect

of adjusting the damper weight ratio on a hexagonal base steel dome structure subjected to different vibrations.

Linear time history analysis is carried out using SAP2000 under sinusoidal ground acceleration as well as scaled-down El Centro earthquake of 1940. Static loads and base excitation vibrations adopted in this study are:

Load case 1: Transverse static point load at the dome apex.

Load Case 2: Base sinusoidal excitation.

Load Case 3: Base scaled-down El Centro earthquake.

All loads in both numerical and experimental tests are applied in elastic range and the results are compared in graphical figures.

1.5 Assumptions and Conditions

1. The structure behaves elastically.
2. Deflection are small.
3. Only unilateral base excitation is considered.
4. The analysis is based on six degree of freedom per joint.
5. The dome supports are fixed.
6. Natural vibration loading is based on a horizontal load applied at the dome apex and then released.
7. All connections in the ribbed dome are welded.

2. EXPERIMENTAL STUDY

2.1 Material Properties

The experimental study includes studying the ribbed dome response under a gradually increasing static load, natural vibration, sinusoidal base excitation, and scaled-down 1940 El Centro earthquake. The ribbed dome was fabricated by welding No. 2 steel rebar. The total self-weight of the dome structure is 9.7 lbs. and the unit weight of the steel equal to $0.274 \text{ lb. / inch}^3$. To determine the Young's modulus, a bending test was conducted on No. 2 rebar used to construct the dome and its value found to be 28213.7 ksi.

2.2 Test Set-up and Procedure

The way that the dome was constructed and the accelerometers attached to the structure are presented in this part. Figure 16 shows an isometric view of the ribbed dome and its six fixed support locations. Figure 17 represent where the accelerometers are placed. Since the apex has the maximum acceleration and displacement, it is selected to be the benchmark to conduct the comparison in the rest of this study. Figure 18 show a picture of the ribbed dome on the shake table.

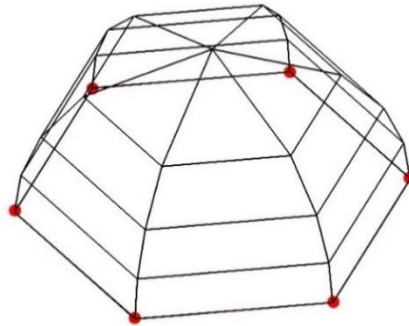


Figure 16: Isometric view of the dome and the base supports locations

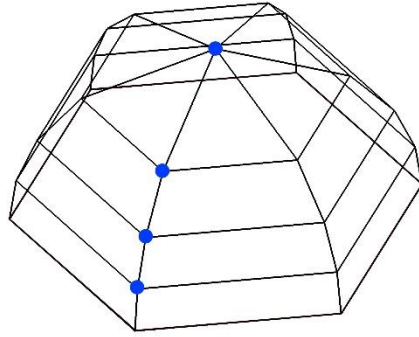


Figure 17: Isometric view of accelerometers locations

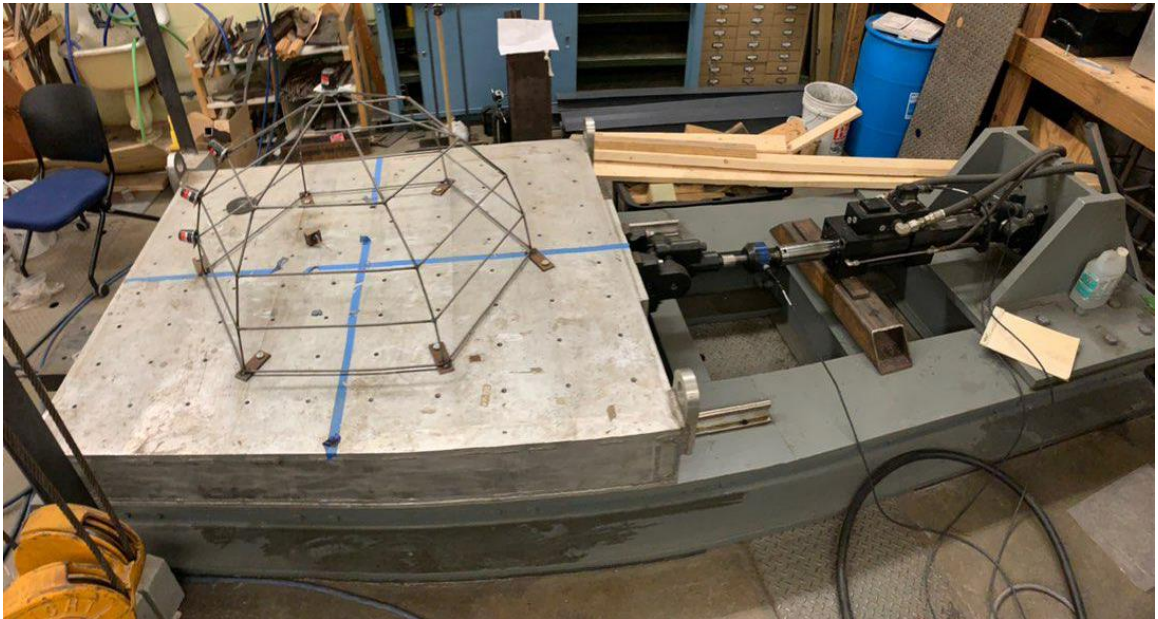


Figure 18: Ribbed dome on shake table

In order to construct the dome, the horizontal elements are labeled based on the height level and the beam-columns are labeled based on rip layers. In Figure 19 the procedure of the labeling is presented in a graphically presented. Properties of all elements presented in the Table 1.

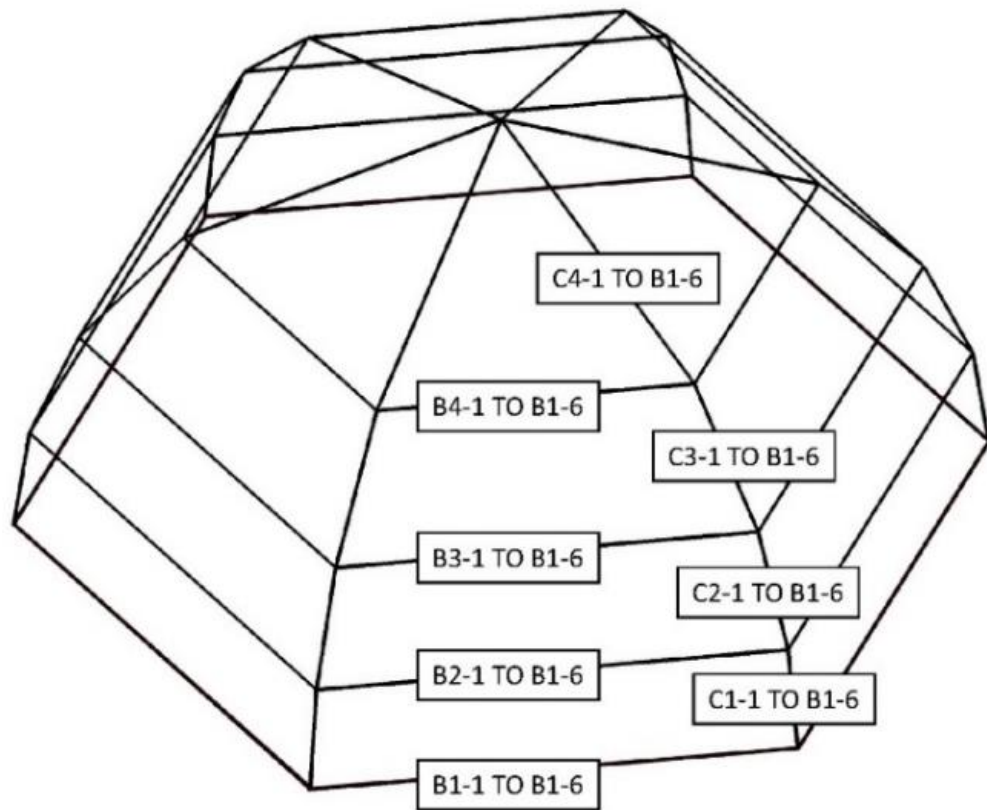


Figure 19: Structure Elements order of labeling

Table 1: Dimension if dome structure elements

| Element | Length (in.) | Element | Length (in.) |
|---------|--------------|---------|--------------|
| B1-1 | 19.68 | C1-1 | 4.75 |
| B1-2 | 19.68 | C1-2 | 4.75 |
| B1-3 | 19.68 | C1-3 | 4.75 |
| B1-4 | 19.68 | C1-4 | 4.75 |
| B1-5 | 19.68 | C1-5 | 4.75 |
| B1-6 | 19.68 | C1-6 | 4.75 |
| B2-1 | 18.87 | C2-1 | 5.12 |
| B2-2 | 18.87 | C2-2 | 5.12 |
| B2-3 | 18.87 | C2-3 | 5.12 |
| B2-4 | 18.87 | C2-4 | 5.12 |
| B2-5 | 18.87 | C2-5 | 5.12 |
| B2-6 | 18.87 | C2-6 | 5.12 |
| B3-1 | 16.93 | C3-1 | 6.31 |
| B3-2 | 16.93 | C3-2 | 6.31 |
| B3-3 | 16.93 | C3-3 | 6.31 |
| B3-4 | 16.93 | C3-4 | 6.31 |
| B3-5 | 16.93 | C3-5 | 6.31 |
| B3-6 | 16.93 | C3-6 | 6.31 |
| B4-1 | 12.62 | C4-1 | 11.81 |
| B4-2 | 12.62 | C4-2 | 11.81 |
| B4-3 | 12.62 | C4-3 | 11.81 |
| B4-4 | 12.62 | C4-4 | 11.81 |
| B4-5 | 12.62 | C4-5 | 11.81 |
| B4-6 | 12.62 | C4-6 | 11.81 |

To demonstrate the length of the elements, two dimensional plan views of each level are presented in the Figure 21. It can be added that the far left is the ring located on the base and the far right is the highest ring of the system. Figure 20 shows the plan view of the hexagonal ring sub-structures' welded at various level of the dome structure to the ribs.

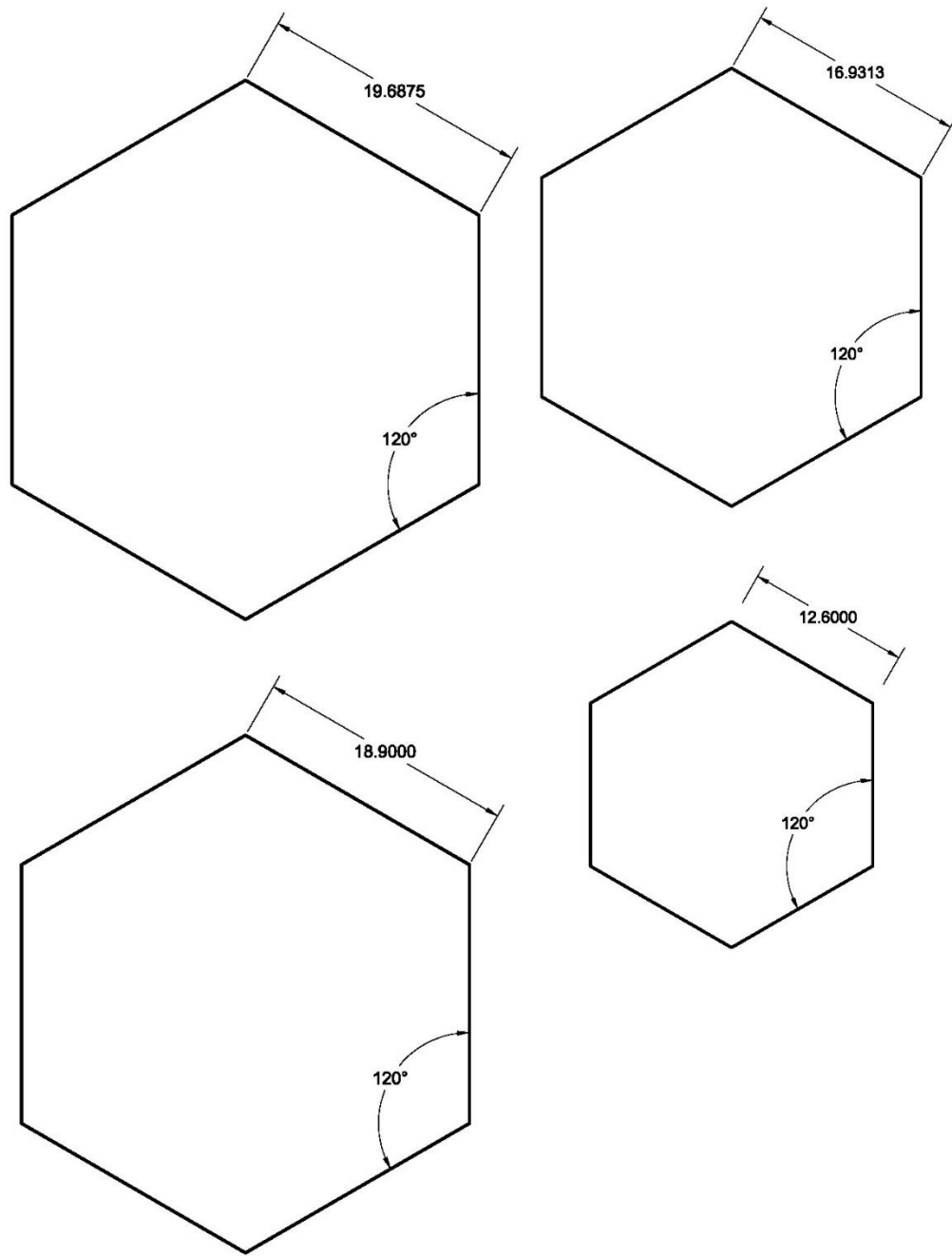


Figure 20: Plan view of dome rings

2.2.1 Static Test

The static test on the dome is conducted by applying a horizontal static point load in increments at the apex and the deflection measured with a dial gauge also attached to the apex. Figure 21 shows the static test setup.

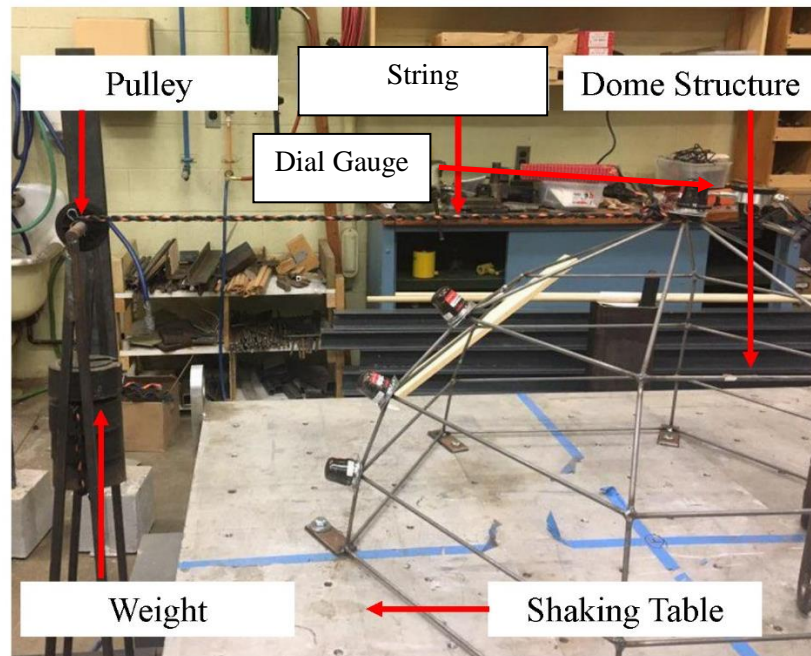


Figure 21: Structure load-deflection test set up.

Table 2 presents the load and deflection data. Figure 21 shows the experimental load deflection relation.

Table 2: Exp. load deflection test results

| Load (kg) | Load (lb.) | Deflection (in.) |
|--------------|---------------|---------------------|
| 0 | 0 | 0 |
| 2 | 4.4 | 0.007 |
| 4 | 8.8 | 0.013 |
| 6 | 13.2 | 0.021 |
| 8 | 17.6 | 0.027 |
| 10 | 22.0 | 0.034 |

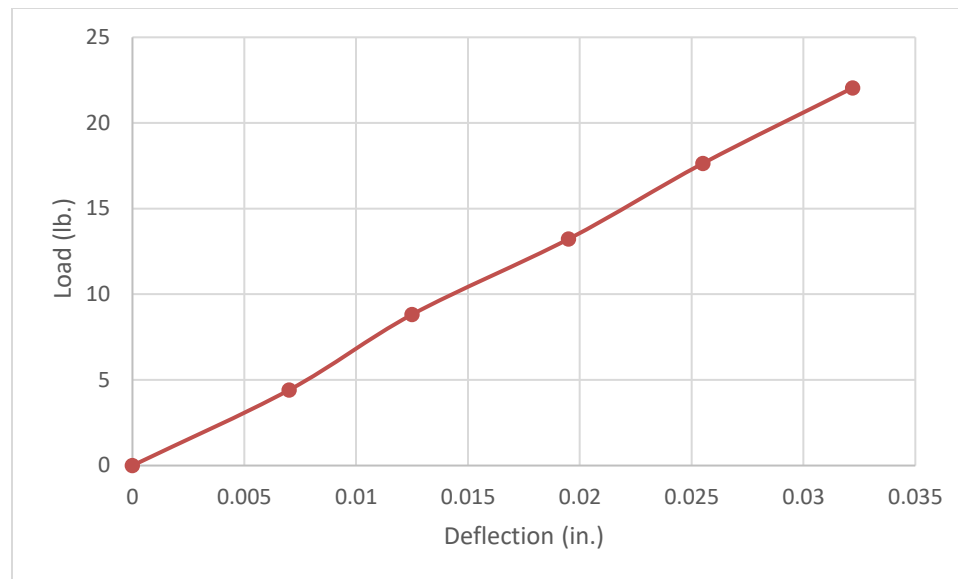


Figure 21: load-deflection relation of experimental test

2.2.2 Vibration Tests

2.2.2.1 Natural Vibration Test

After structure is attached and fixed to the base, a string is tied to the top of the dome structure. When a transverse load of 8 kg (17.6 lb.) is applied to the structure, the string is cut off and the structure starts to vibrate. The structure vibrates until it returns to its initial position and stops vibrating.

Figure 23 presents the natural vibration of the dome in the experimental test. It is showing how the system responds to the load and how it turns back to its initial point. Since the structure is rigid and the supports are all fixed, the number of the cycles of vibration in one second is a large value. In this model, the frequency is equal to 24 cycles per second.

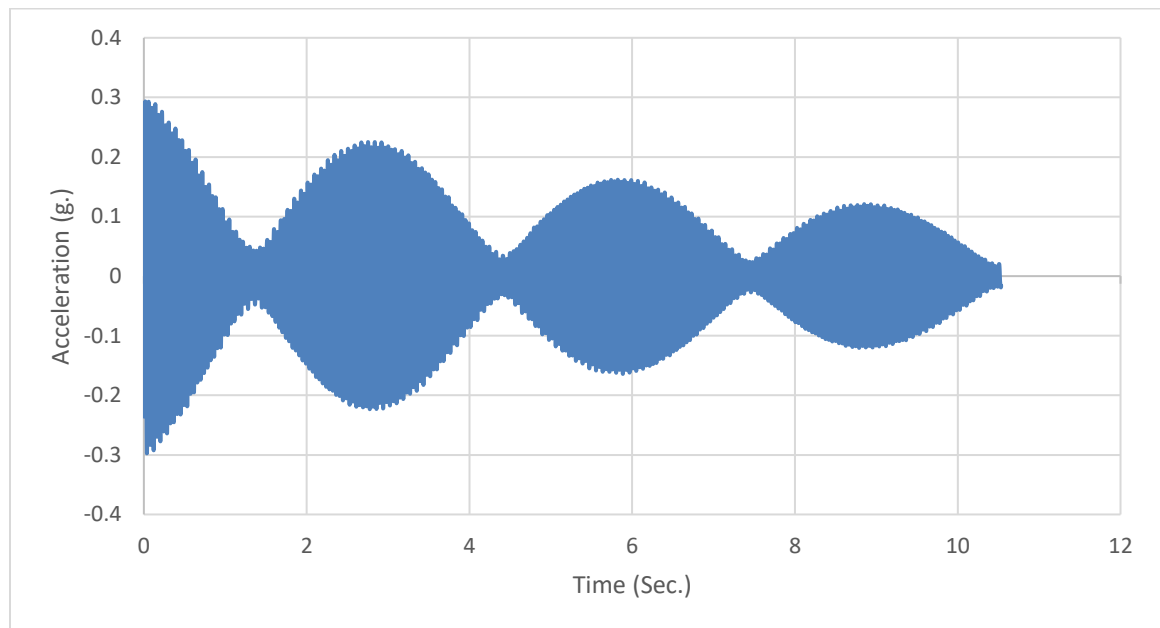


Figure 22: Experimental acceleration vs. time relation for free vibration test

2.2.2.2 Base Excitation Test

To do the dynamic tests, Old Dominion University civil engineering shaking table is utilized. The Structures/Earthquake Engineering Laboratory has a 5' x 4' shaking table, a reaction floor, a servo controlled MTS dynamic testing system with actuator capacities varying from 500 lbs. to 100 kips.

Four Lord G-Link-200 accelerometers where the locations described in the previous part; attached to the dome structure.

To control and apply the sinusoidal and El Centro earthquakes structural lab computer is utilized which is connected to the actuator and shaking table to provide the intended earthquake.

The collected data have noises. In order to have an accurate and smooth data set up, noises are canceled from the data with the Mat Lab code provided here.

```
dt=1/512;  
  
fs    = 512 ;  
  
fc    = 15 ; %50      % Hz  
  
Filter_order=6 ;  
  
[B, A]= butter(Filter_order,2*fc/fs,'low');  
  
%[b_acc,a_acc]=butter(Filter_order_acc,2*pi*cut_off_freq_acc,'s'); This  
%kind of filter should be used just in the main codes on simulations since  
%we are applying analog filter, where Wn should be in radians and 's'  
%represents the 'lowpass', while for post processing, the digital filters
```

%should be applied where W_n should be between 0 and 1 and we should define type of filter; Please read the Butter filter specifications!

```
node1f=filtfilt(B,A,node1);
```

```
node2f=filtfilt(B,A,node2);
```

```
node3f=filtfilt(B,A,node3);
```

```
node4f=filtfilt(B,A,node4);
```

The response of the four nodes on the structure subjected to the sinusoidal vibration are presented in the Figure 26, 27, 28, and 29. In figure 25 the locations of the nodes are presented. The green lines are the filtered data and the black line is the pure data which comes from the accelerometer.

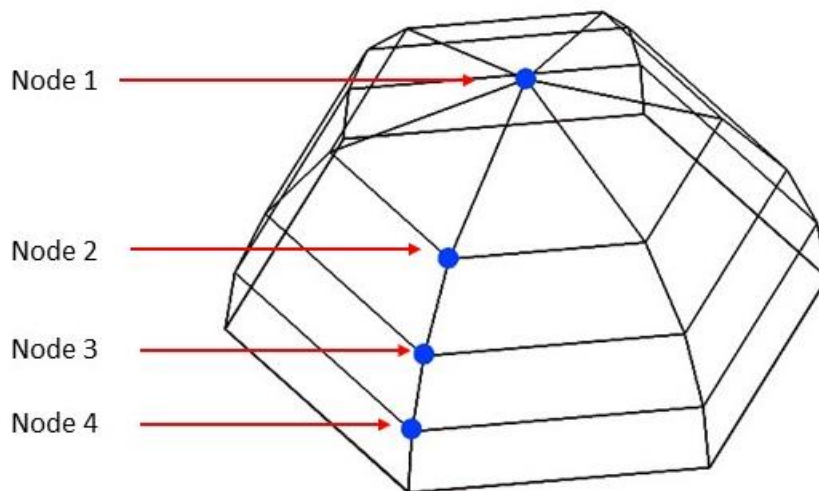


Figure 23: Accelerometers Locations on the dome structure

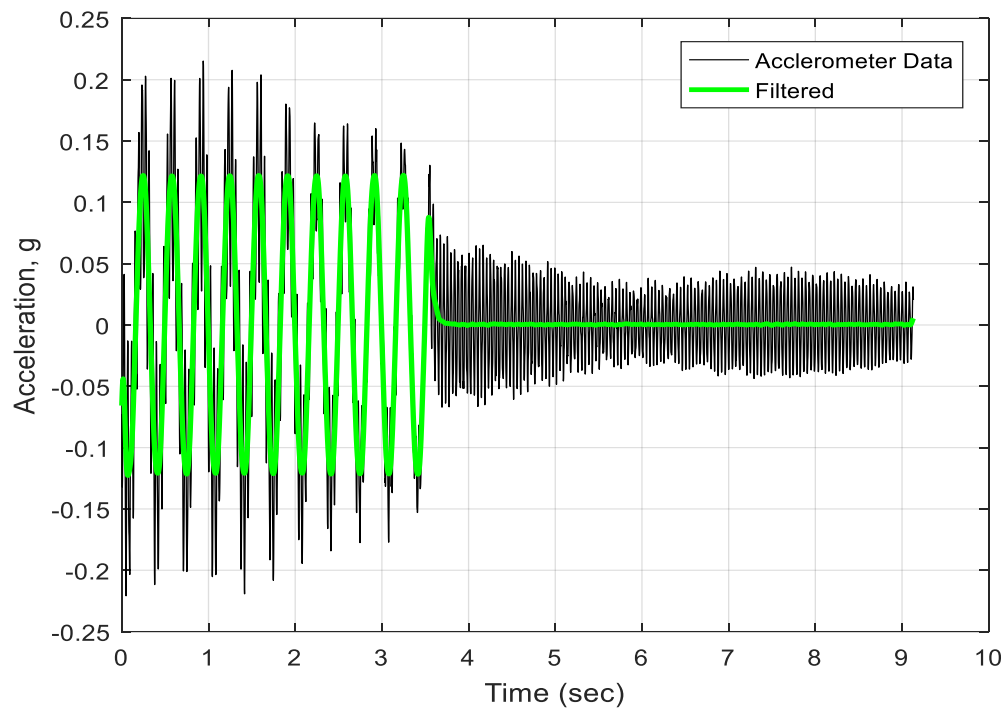


Figure 24: Exp. Acceleration vs. time relation of Node 1 in sinusoidal base excitation

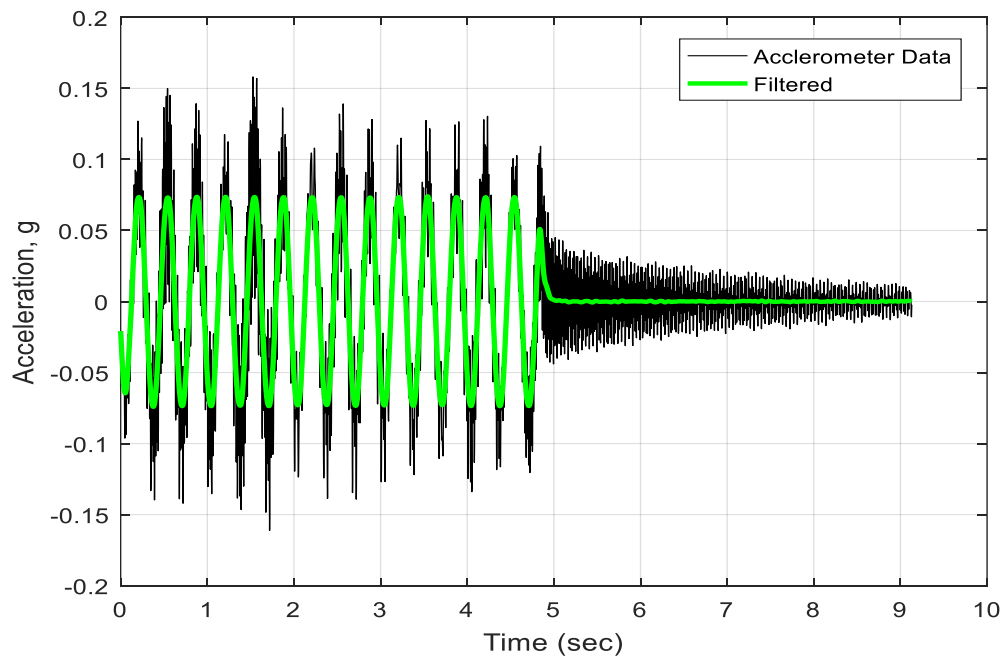


Figure 25: Exp. Acceleration vs. time relation of Node 2 in sinusoidal base excitation

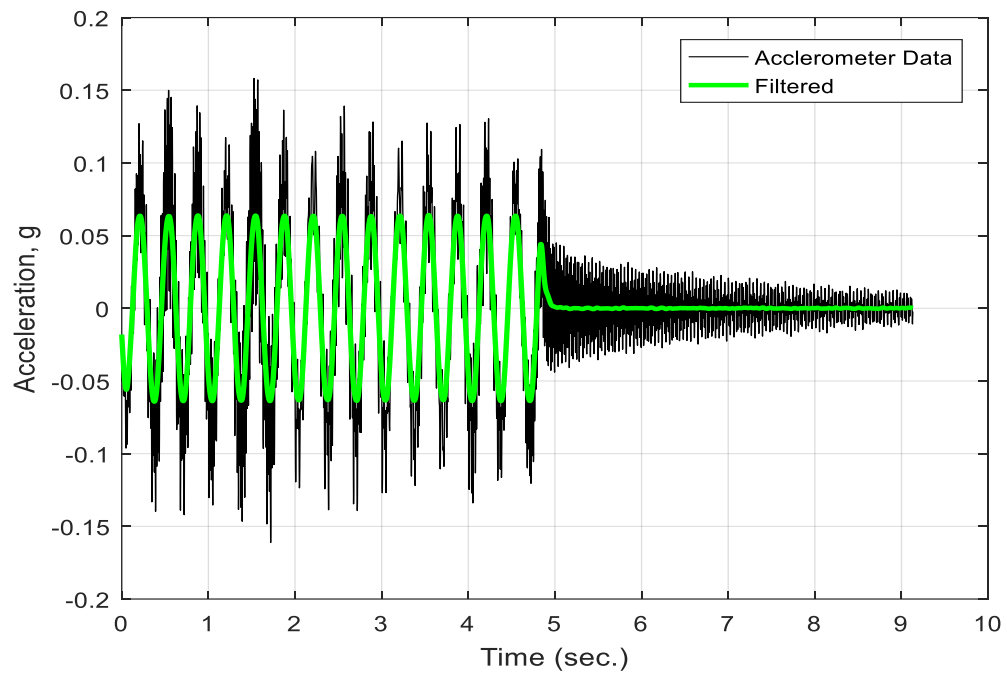


Figure 26: Exp. Acceleration vs. time relation of Node 3 in sinusoidal base excitation

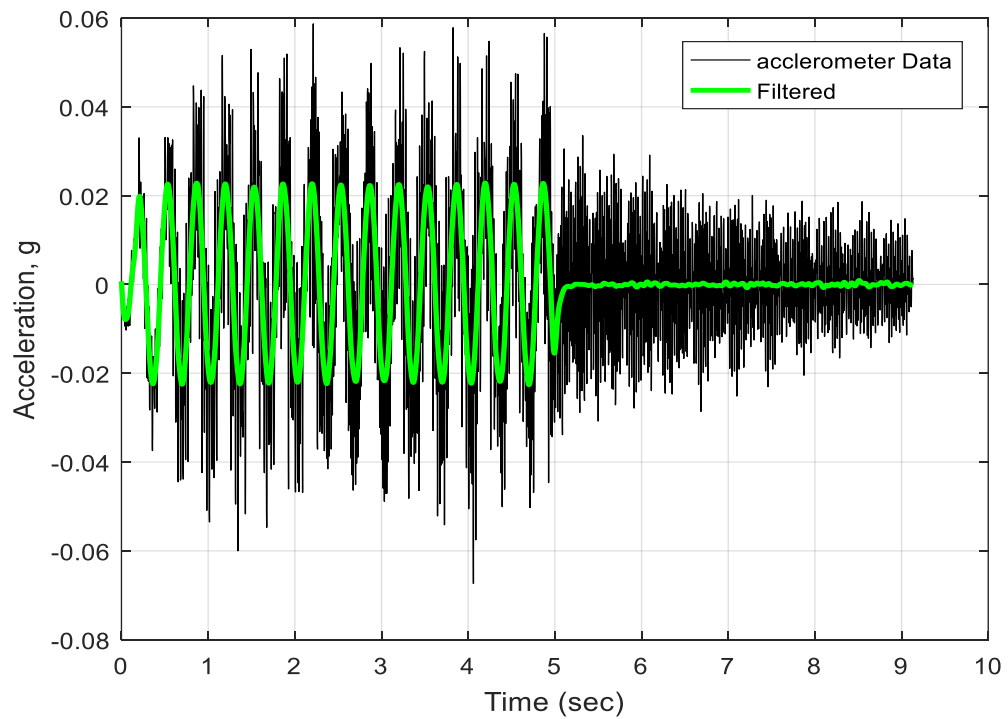


Figure 27: Exp. Acceleration vs. time relation of Node 4 in sinusoidal base excitation

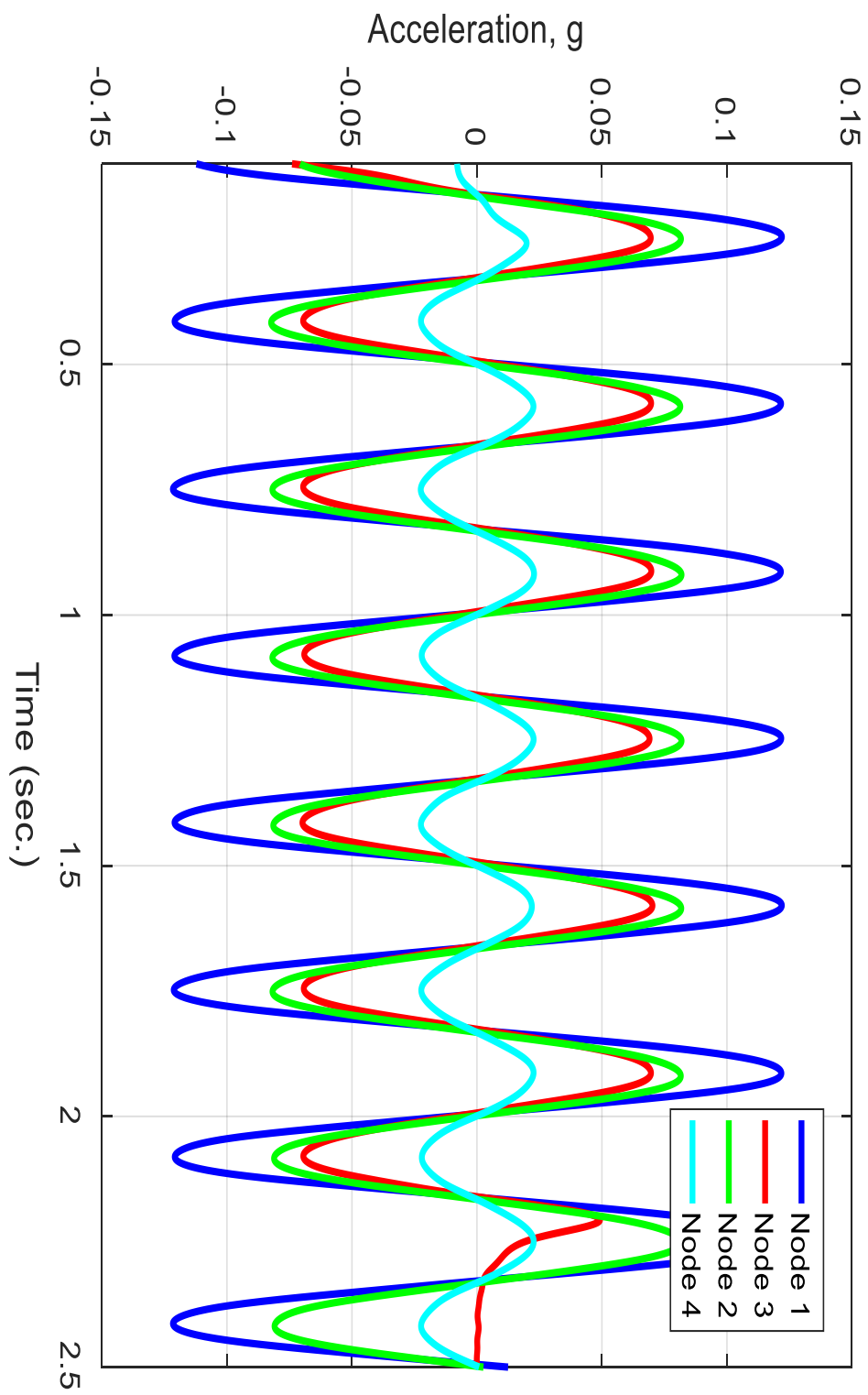


Figure 28: Experimental acceleration vs. time relation comparison

As it is showing in Figure 30 the acceleration of the structure is decreased as the nodes get closer to the shake table.

The second type of the vibration that the structure is subjected to is the scaled-down El Centro earthquake of 1940. The displacement amplitude of the El Centro is scaled-down by 300%. The response of the system at the apex point is presented in Figure 31.

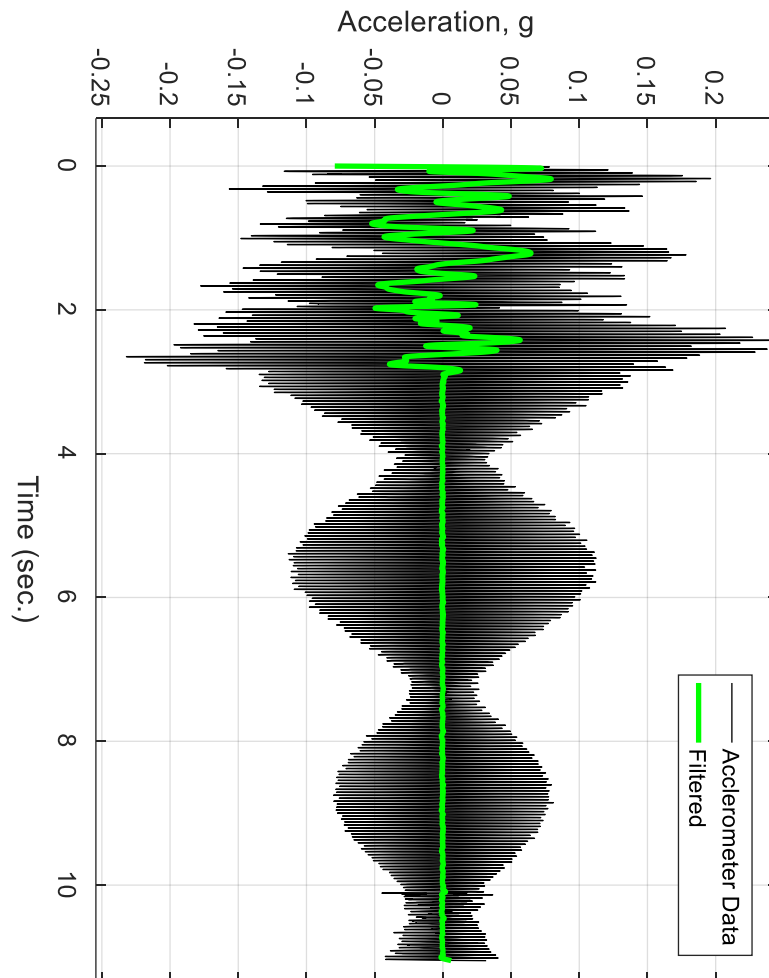


Figure 29: Experimental El Centro earthquake Response of the dome structure

Unidirectional Forcing function versus time, Displacement versus time, and acceleration versus time relations of the shaking table inputs are as follows.

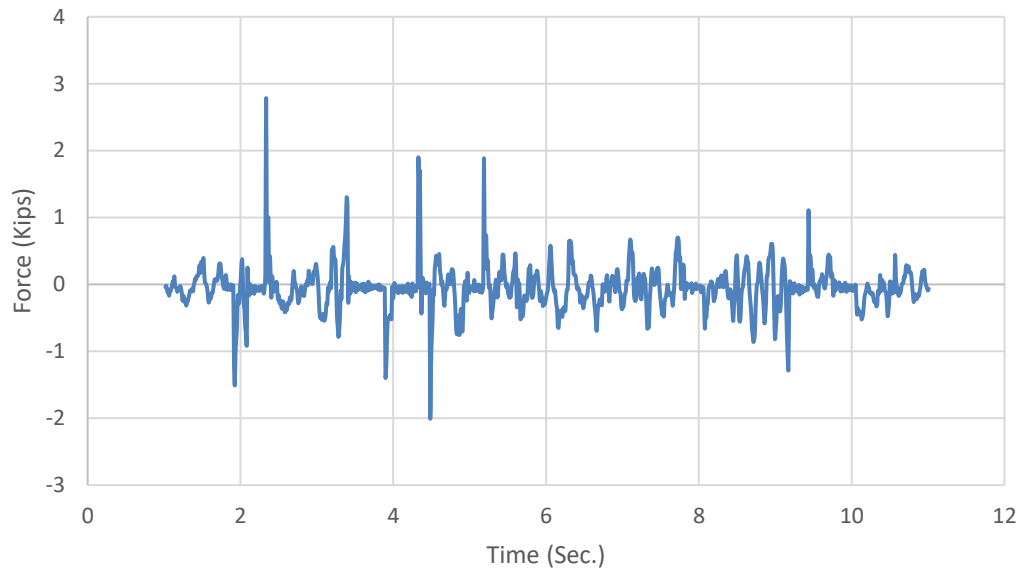


Figure 30: Unidirectional Forcing function vs. time relation of the EL Centro Earthquake of 1940

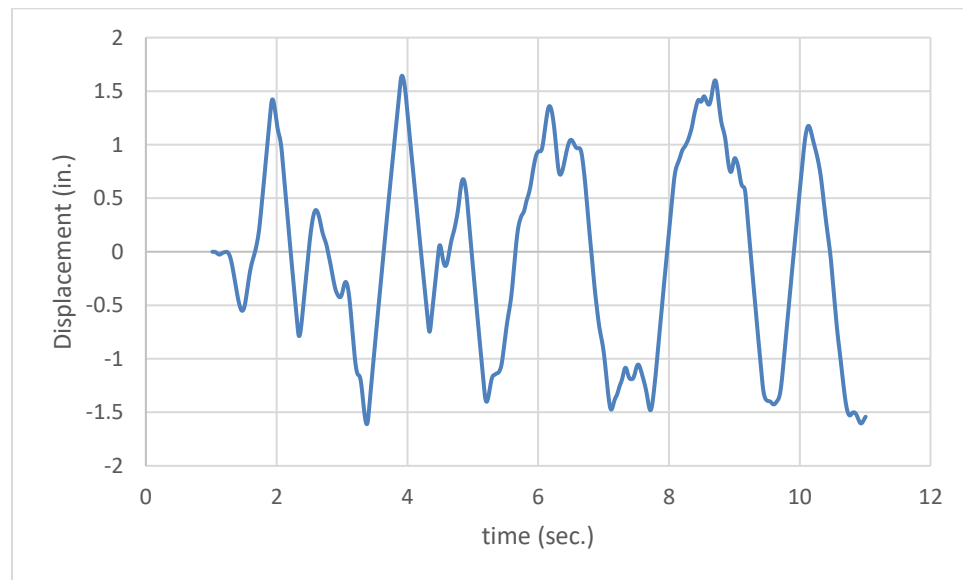


Figure 31: Displacement vs. time relation of the EL Centro Earthquake of 1940

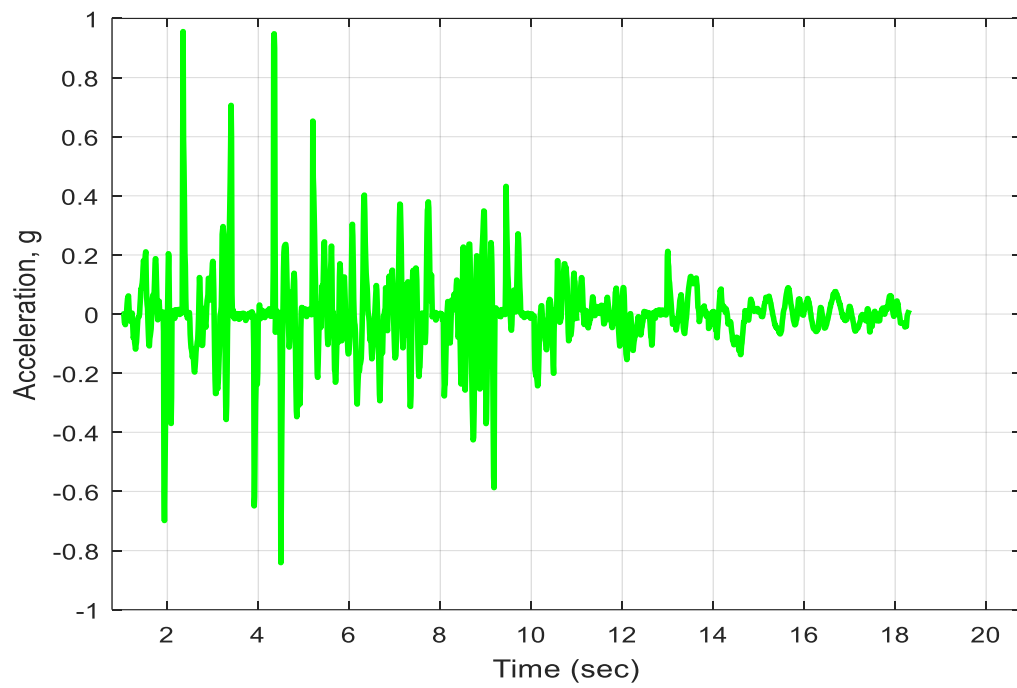


Figure 32: Acceleration vs. time relation of the EL Centro Earthquake

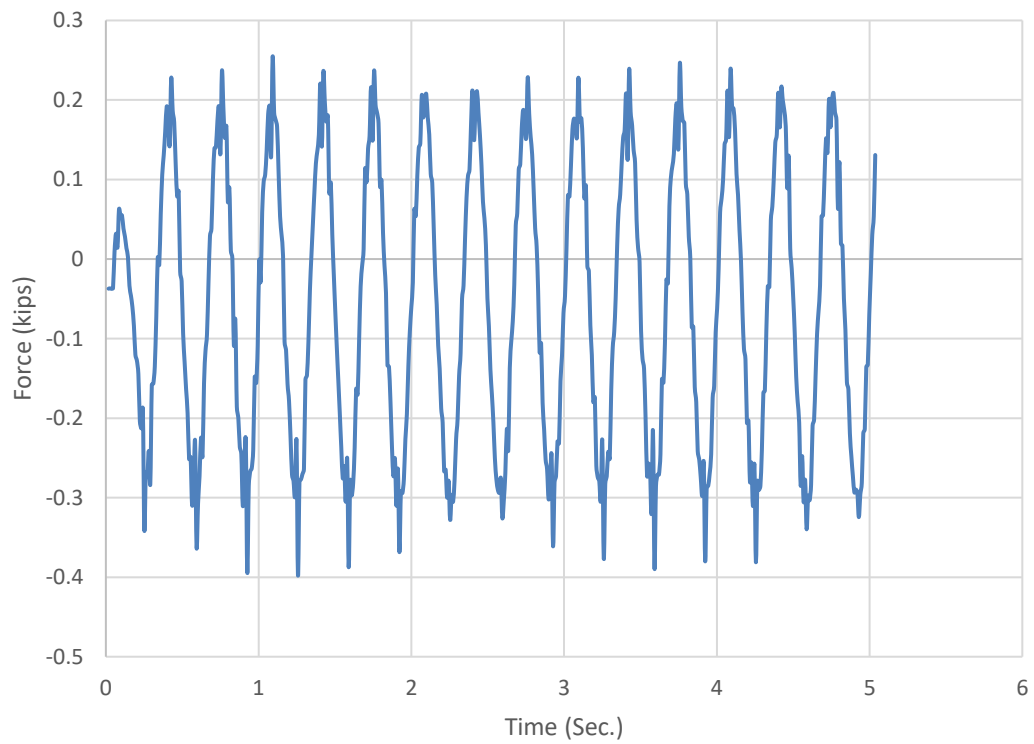


Figure 33: Unidirectional Forcing function vs. time relation of the sinusoidal vibration

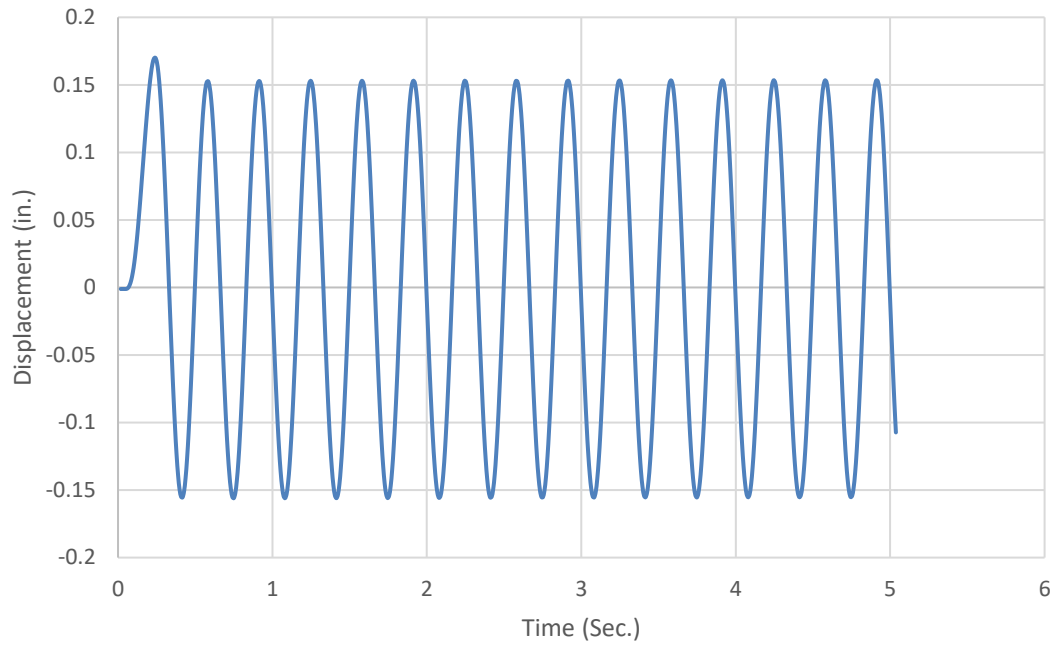


Figure 34: Displacement vs. time relation of the sinusoidal vibration

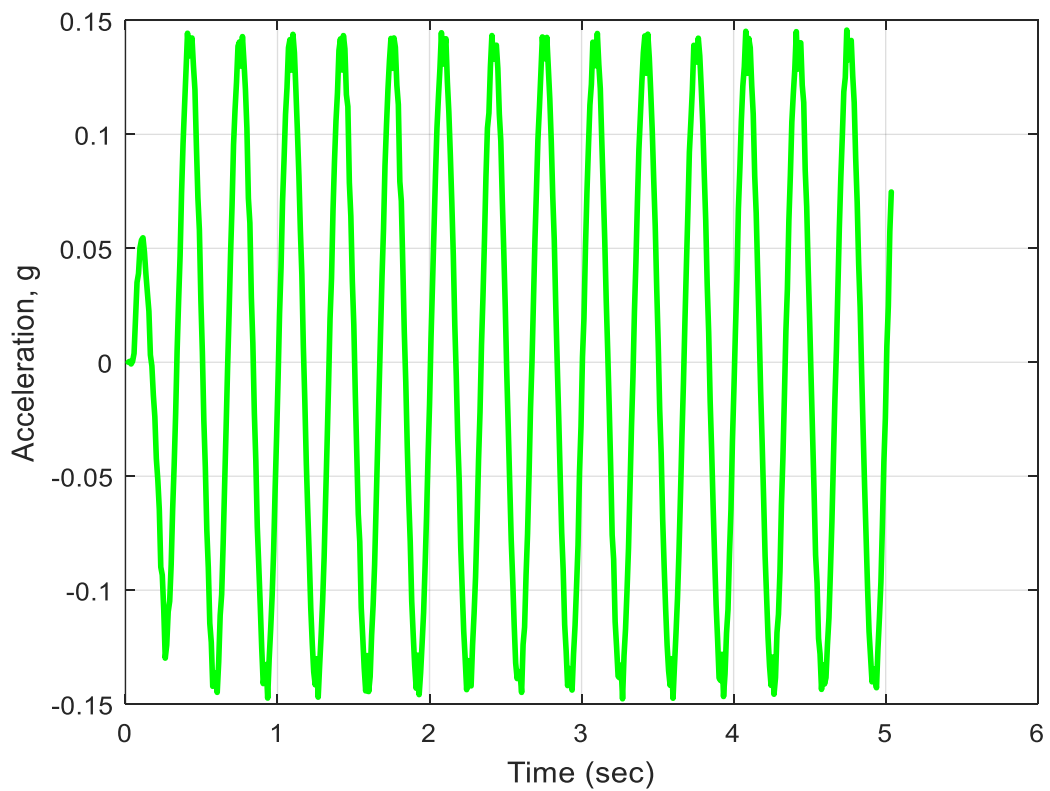


Figure 35: Acceleration vs. time relation of the sinusoidal vibration

3. THEORETICAL STUDY

3.1 Methodology

The equation of motion for the model subjected to external dynamic force $R(t)$ can be written as:

$$M\ddot{U} + C\dot{U} + KU = R(t) \quad (\text{Equation 1})$$

Here the external force $R(t)$ can be distributed into three mechanisms of the structure. First, by the stiffness component, second by damping component and third by mass component. So the dynamic response of the structure to the excitation can be expressed by the displacement $U(t)$, velocity $\dot{U}(t)$, and acceleration $\ddot{U}(t)$. Where M is mass matrix of the frame model, C is global matrix of the frame model, K is global stiffness of the frame structure and U is global nodal displacement vector.

Tuned mass damper is like a mass which is attached to a structure where the frequency of the damper is tuned to a particular structural frequency, so that when that frequency is excited, the damper will response out of phase with the structural motion. Based on the motion equation we can rewrite the equation as:

$$[M]\{\ddot{u}\} + [c]\{\dot{u}\} + [k]\{u\} = \{R(t)\} \quad (\text{Equation 2})$$

Natural frequency of the structure and the damper are:

$$\omega = \sqrt{\frac{k}{m}} \quad (\text{Equation 3})$$

$$\omega_d = \sqrt{\frac{k_d}{m_d}} \quad (\text{Equation 4})$$

And:

$$\xi = \frac{c}{2m\omega} \quad (\text{Equation 5})$$

$$\xi_d = \frac{c_d}{2m_d\omega_d} \quad (\text{Equation 6})$$

The mass ratio which is the mass of the damper to the structure mass presented by Υ which is equal to:

$$\Upsilon = \frac{m_d}{m} \quad (\text{Equation A.7})$$

m_d is mass of damper, C_d is damping of damper, K_d is stiffness of damper.

3.2 Numerical Modeling

3.2.1 SAP Modeling

A hexagonal base ribbed dome structure with the height of 1 foot and 8 inches and with 3 rings in the elevation is designed and modeled in the SAP. In Figure 38 an isometric view of the SAP model is presented;

The modeling procedure for the dome system is:

1. Draw grid lines as a reference based on the structure dimensions.
2. Draw actual elements on the grid.
3. Create a quarter of an inch diameter steel rebar cross section material.
4. Assign the material to the elements.
5. Create a weld joint condition.
6. Assign the joint condition to the structure.
7. Assign the fixed condition to the base joints.
8. Loads:
 - 8.1. For static test apply joint force at the apex of the structure
 - 8.2. For the sinusoidal base excitation; create a sinusoidal time history load case based on the calculated frequency, displacement and number of cycles.
 - 8.3. For El Centro base excitation; import an excel file of the El Centro displacement versus time relation and consider the scale.
9. To find the natural frequency; run the program just with the modal load case.
10. To find the acceleration versus time relation for the sinusoidal and El Centro; First, run the dead, modal, and intended vibration load cases. Then, select the apex point and

draw graph of acceleration versus time. SAP also provide the option to export the data in excel version.

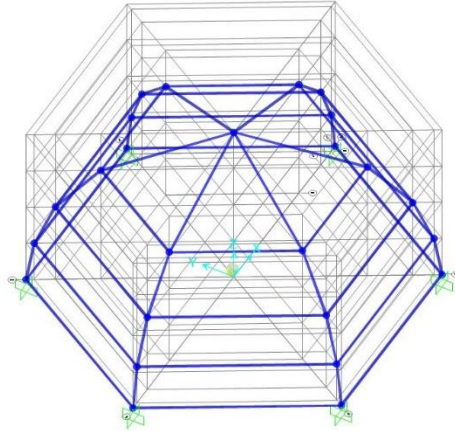


Figure 36: Isometric view of the numerical model of the dome

3.2.1 Static Test

Load-deflection test is the primary test that can cast light on the properties of the system, where the lateral stiffness of the structure can be calculated. The tip of the structure is subjected to static point load while the deflection collected from the analysis results; point load gradually increases to reach 22 lb. static load.

The following graph represent the load-deflection graph of the experimental laboratory test result and the numerical results.

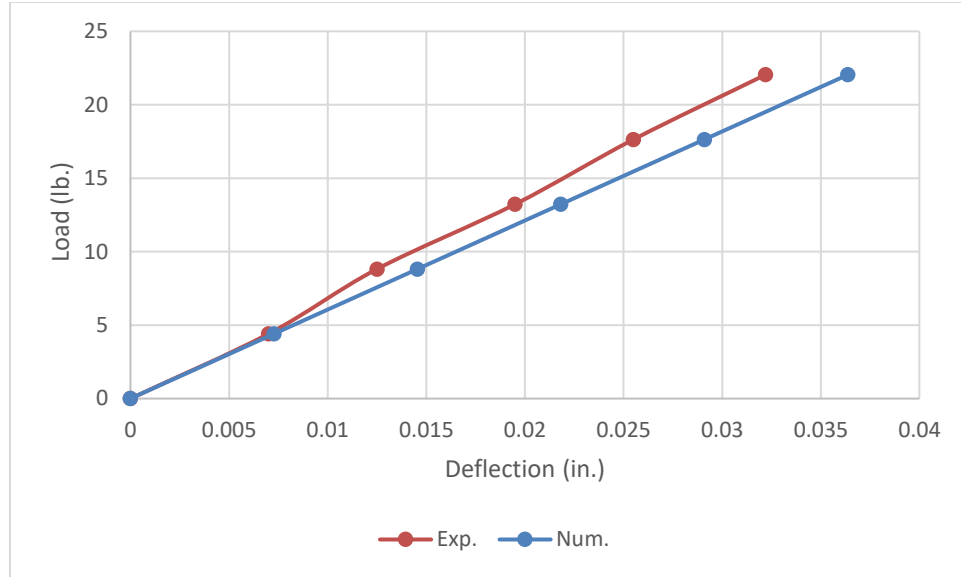


Figure 37: load-deflection relationship of both experimental and numerical

Table 3: Exp. And Num. load deflection tests result

| Load (kg) | Load (lb.) | Deflection (in.) | SAP2000 (in.) |
|-----------|------------|------------------|---------------|
| 0 | 0 | 0 | 0 |
| 2 | 4.4 | 0.007 | 0.0072 |
| 4 | 8.8 | 0.013 | 0.0145 |
| 6 | 13.2 | 0.021 | 0.0218 |
| 8 | 17.6 | 0.027 | 0.0290 |
| 10 | 22.0 | 0.034 | 0.0363 |

The maximum difference between the experimental and the numerical model is 0.00609 inches. Which is less than 6%. The average stiffness of the system from experimental and numerical is equal to 0.58 kips/in. for numerical and 0.61 kips/in. for experimental.

3.2.2 Vibration Tests

3.2.2.1 Natural Vibration test

Free vibration test also is conducted on the sap model. And the results are presented in this section. Logarithmic increment method is also employed in order to figure the damping of the system.

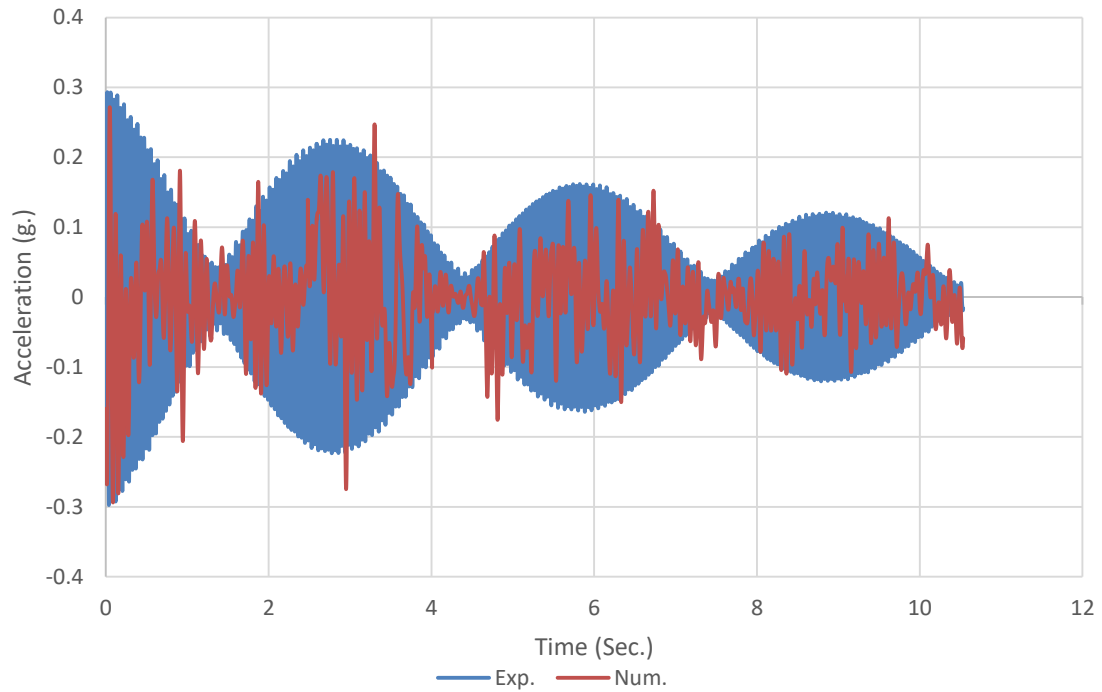


Figure 38: Exp. And Num. free vibration acceleration vs. time relation of the

Figure 39: Free vibration acceleration vs. time relation of both exp. And Num. (Call out)

Table 4: Logarithmic Increment results of Exp. and Num.

| | 1st point | 2nd Point | 3rd Point | 4th Point | Dampin g (1st and 2nd) | Dampin g (1st and 3rd) | Dampin g (1st and 4th) |
|------|-----------|-----------|-----------|----------------------|------------------------|------------------------|------------------------|
| Exp. | 0.0391 | 0.0291 | 0.0218 | 0.0152 | 0.047 | 0.046 | 0.06 |
| Num. | 0.0378 | 0.0274 | 0.01917 | 0.01221 | 0.051 | 0.054 | 0.061 |
| | | | | Exp. Damping Average | 5.1% | | |
| | | | | Num. Damping Average | 5.5% | | |

The logarithmic equation that is used to find the damping is:

$$\zeta = \frac{1}{2\pi j} \log \frac{\ddot{u}_i}{\ddot{u}_{i+j}}$$

The system is now ready to be subjected to sinusoidal and El Centro earthquake vibrations model. Figure 43 shows the acceleration versus time relation of the dome structure with 10% mass damper and without damper.

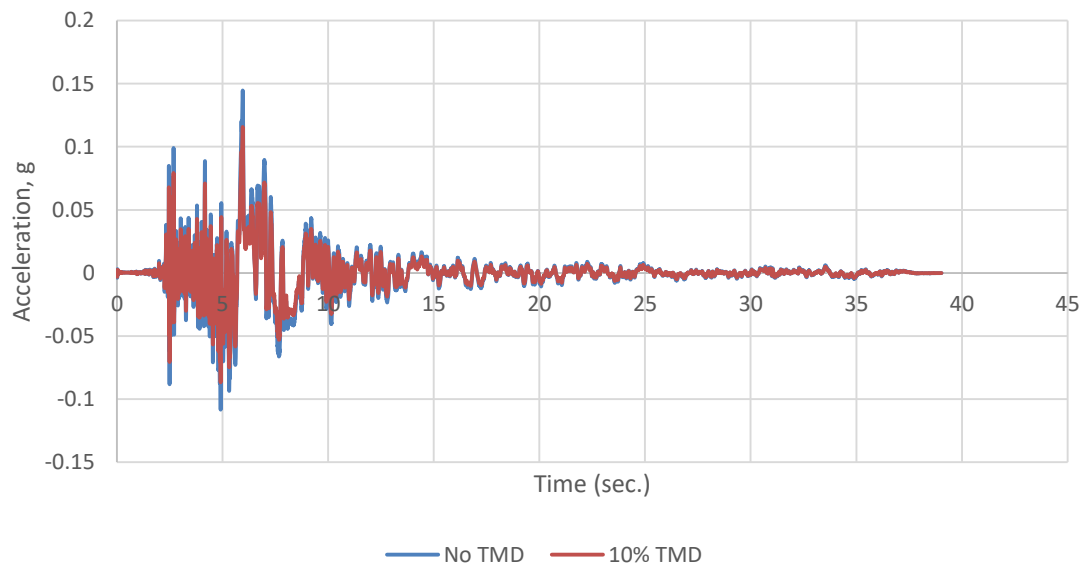


Figure 40: Acceleration versus time relation of the dome numerical model with 10% and without TMD

3.2.2.1 Geometry Effectiveness Test

As it is mentioned in the previous part the domed structure geometry effects the structural response. In order to grasp the influence of the geometry of the curved shape on the maximum acceleration; a hexagonal structure with the same amount of material and same height modeled and subjected to the El Centro earthquake. The systems modeled with the same base geometry, and identical height of the dome; but the only difference is in the angle of vertical members that they are all vertically straight elements. Total weight of the dome system calculated and the cross-section of the hexagonal model modified based on the total mass of the dome. The dome and hexagonal structure subjected to the same El Centro earthquake and the response presented here.

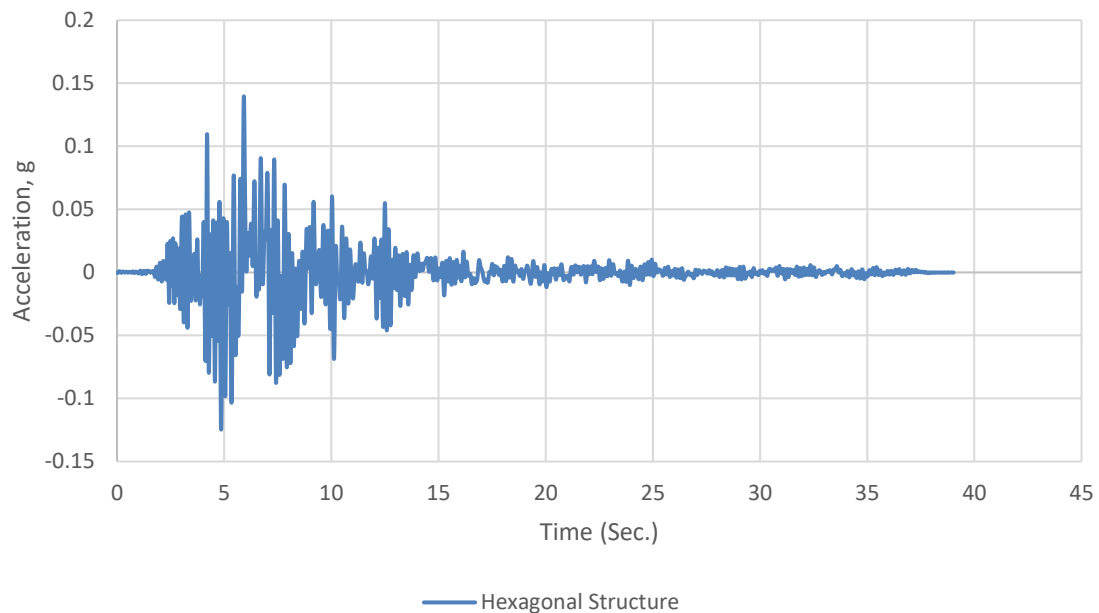


Figure 41: Acceleration versus time relation of numerical study of the hexagonal structure

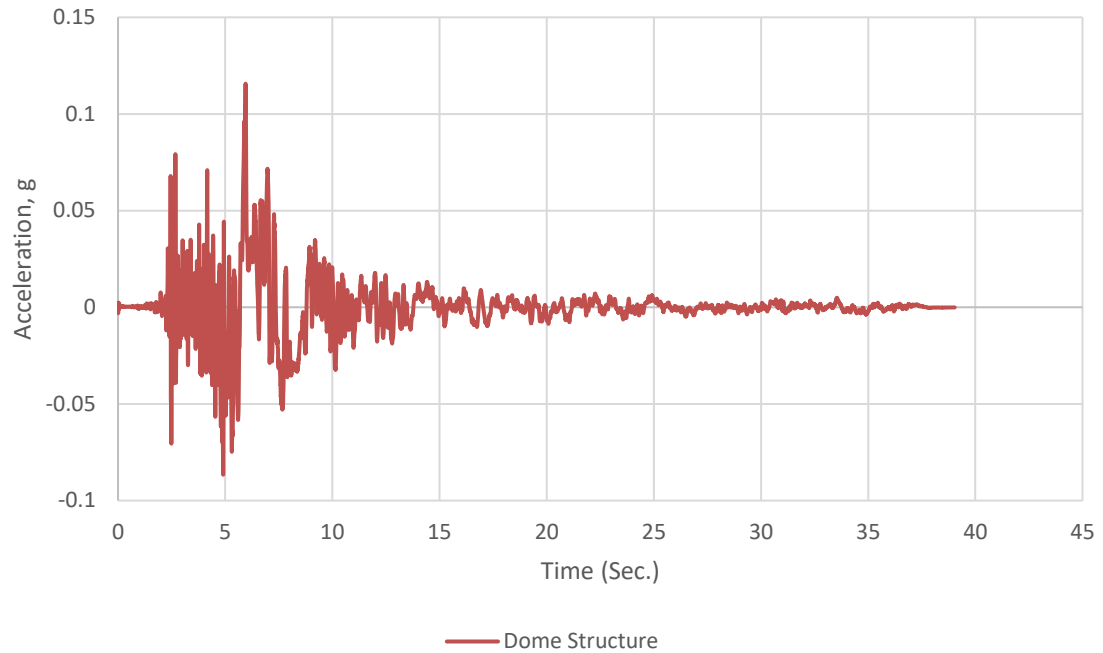


Figure 42: Acceleration versus time relation of the dome numerical model

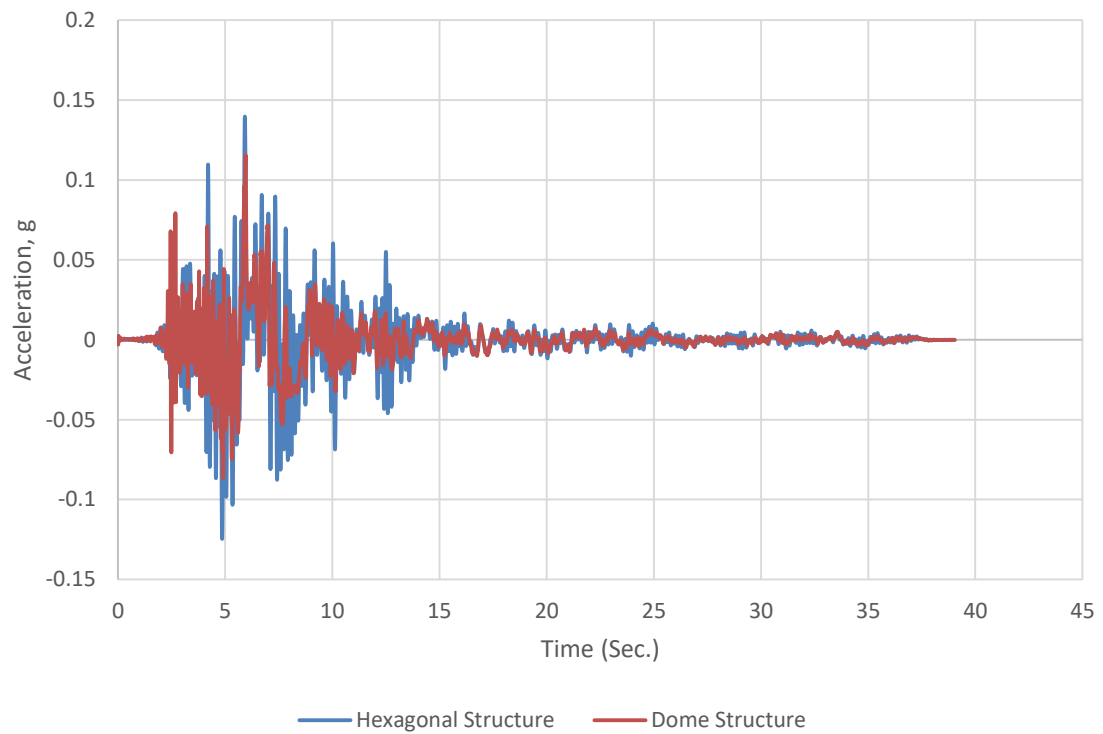


Figure 43: Numerical result of Acceleration versus time relation of the dome structure and hexagonal structure

The Figure 47 shows the 3d view of the hexagonal structure; as it showing the system anchor to the base by the fixed support condition. All joints are modeled in the same condition as we have in experimental set-up.

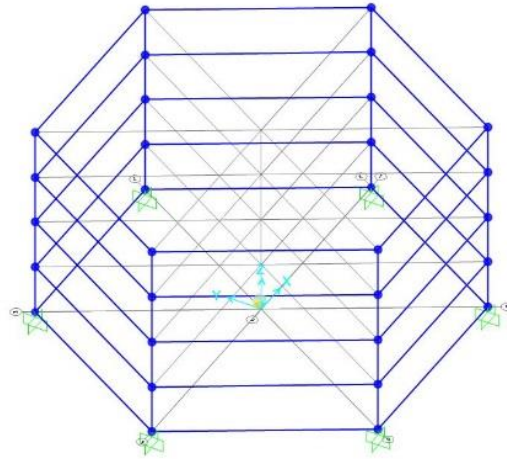


Figure 44: Isometric view of hexagonal SAP model

As it is showing in the Figure 46; the effectiveness of the dome geometry is considerable. It is showing that the maximum acceleration of the system decreased from 4.2 to 3.3 which is 28% decrease in the acceleration amplitude.

3.2.2.2 Base Excitation Test with TMD

The motive of this study is to reduce the response by attaching a tuned mass damper to the structure under sinusoidal loading and also obtain the effect of the mass ratio.

In order to figure the effectiveness of the tuned mass damper, the system subjected to the same sinusoidal vibration with and without damper. First the dome system without damper subjected to the sinusoidal vibration then after; different mass ratio of the TMD modeled and again the system being subjected to the same vibration.

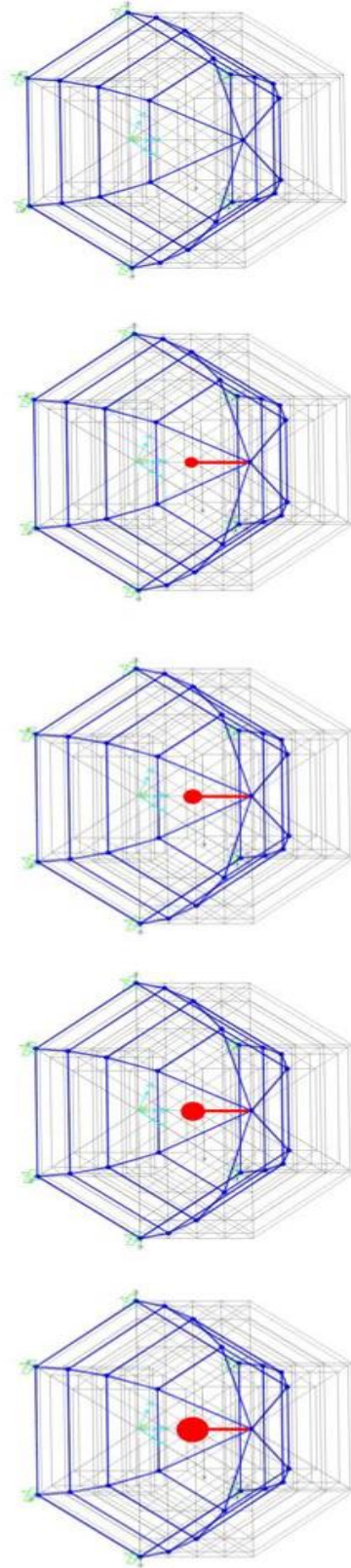


Figure 45: TMD Mass Ratio increment of numerical model

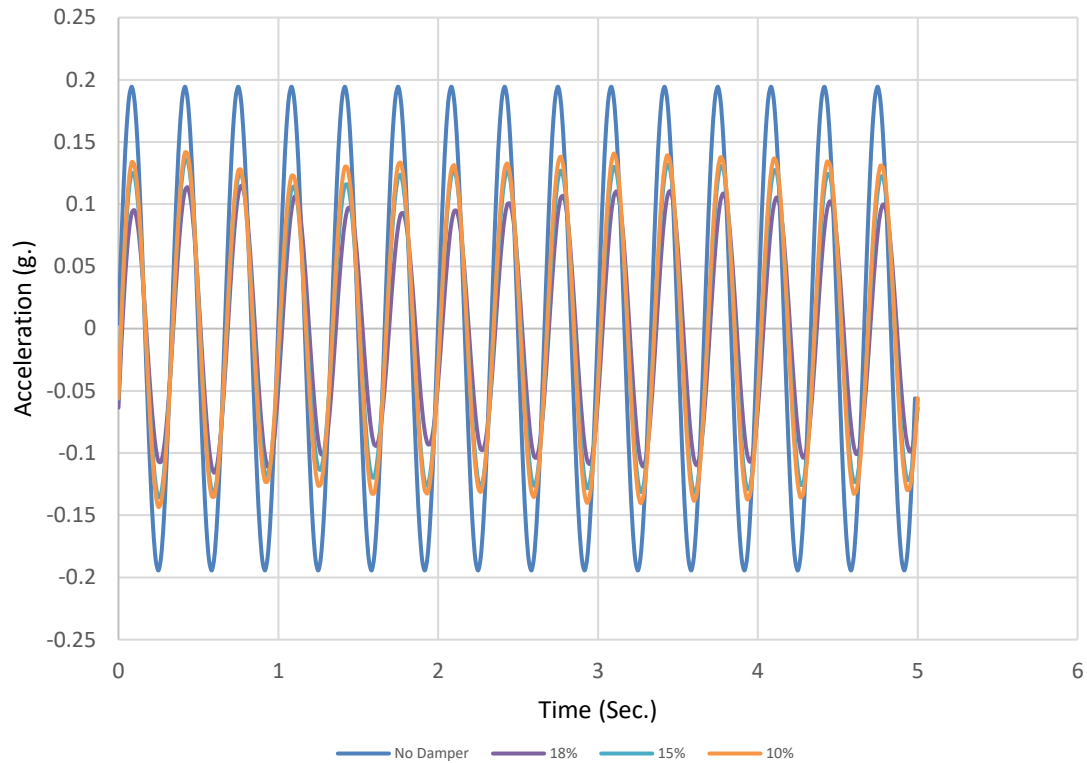


Figure 46: SAP model response of TMD in sinusoidal vibration

A linear sinusoidal vibration of 3 Hz with an amplitude of 0.15 inches and 15 cycles subjected to the system; the blue line represents the acceleration of the structure at the very top point. The orange color line shows the acceleration of the structure tuned with the mass ratio of 10%. It is obvious that the maximum amplitude of the acceleration decreases from 0.19 to 0.13 with this setup. As the mass ratio increases, the maximum amplitude of the acceleration decreases. After 18% as it is showing in Figure 51 the slope of the line becomes close to zero that implemented that the optimize mass ratio for this system is about 18% of the total mass.

In Figure 51 different damper mass ratios studied and presented in the spectrum graph. As it is showing; the maximum acceleration of the system decrease as the mass ratio increases.

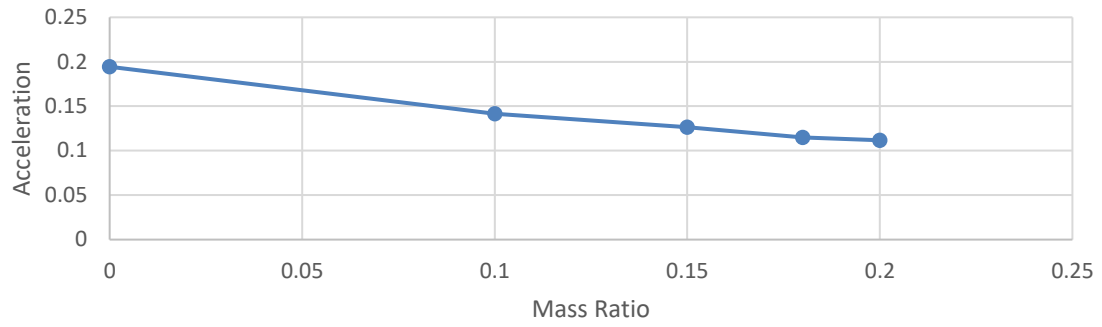


Figure 47: Mass Ratio versus max. Acceleration relation of the numerical dome model

In this section the response of the dome structure to the sinusoidal and El Centro earthquake presented and compared.

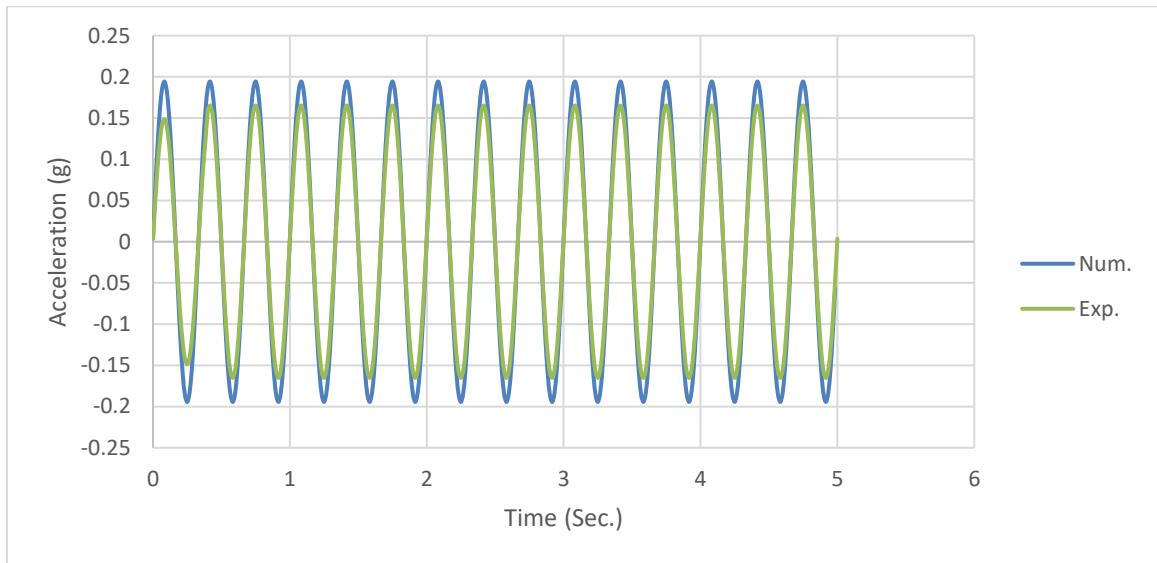


Figure 48: Response of the numerical and experimental dome model to the sinusoidal vibration

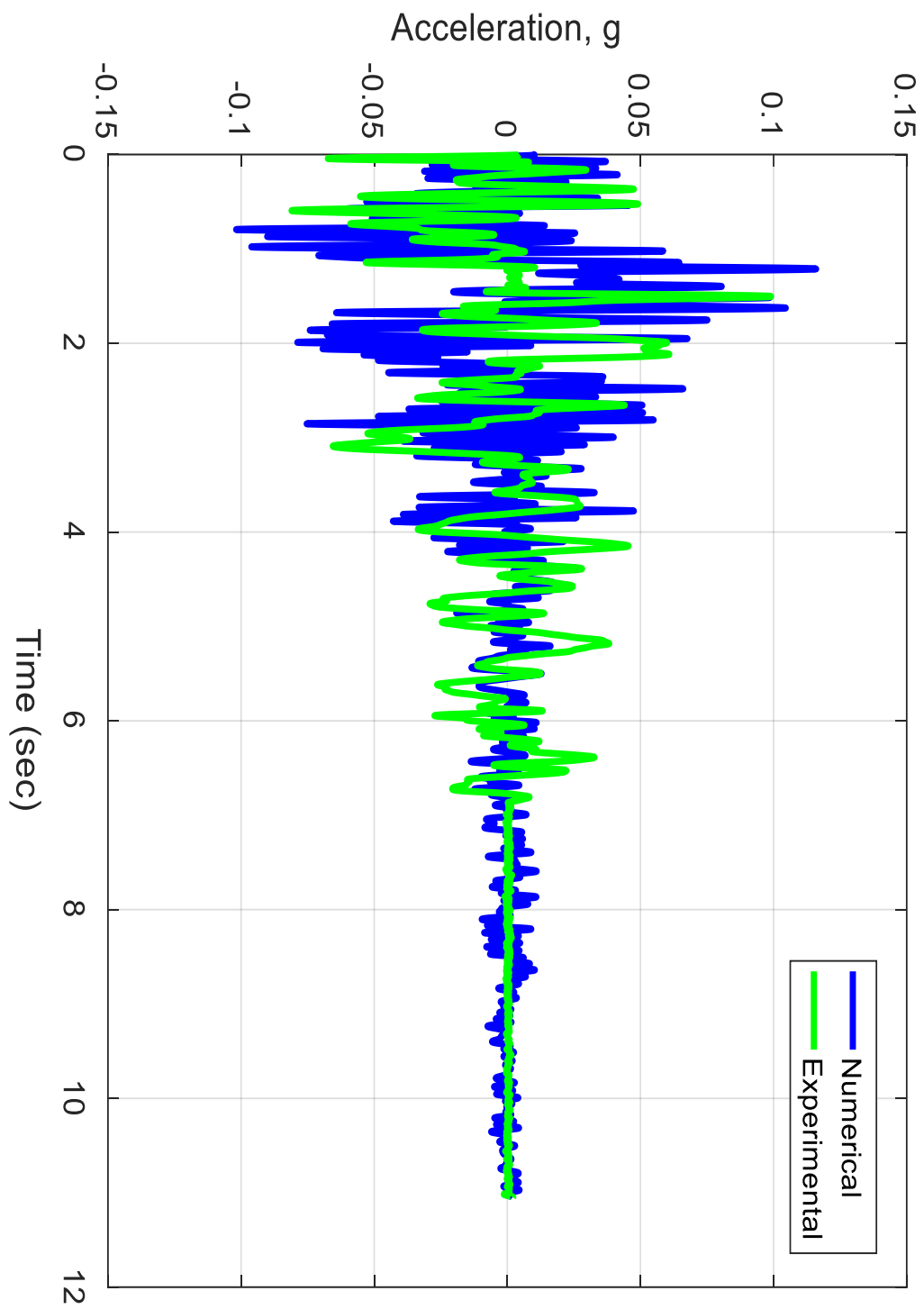


Figure 49: Response of the numerical and experimental dome model to the El Centro vibration

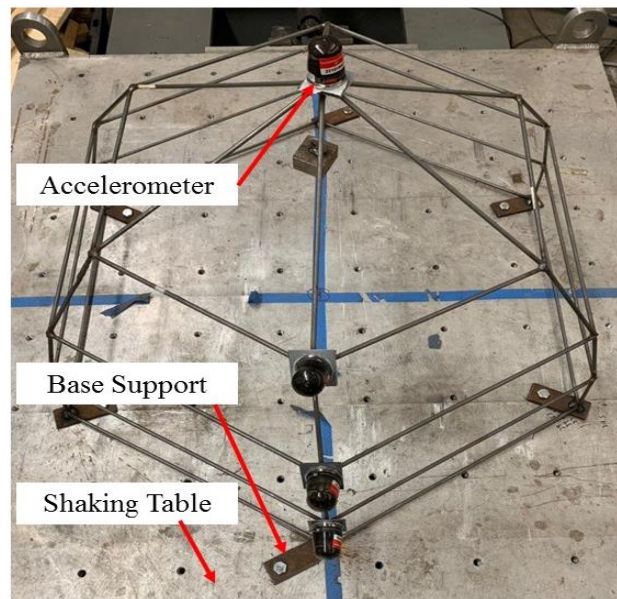


Figure 50: Experimental model set up

Based on the Figure 53 it can be seen that there is a little delay in the experimental data which can be because of the small delay of the shaking table at the beginning point or the human error in collecting data.

4. ARCHITECTURAL DESIGN

4.1 Proposed Architectural Design

An alternative housing system using light steel structure with a thin layer of concrete is proposed for marginal urban and rural areas. The tests in the previous chapter presented showing high ductility and energy dissipation in comparison to other forms.

The concept of the proposed design is to build on the principle of the studied structure but in a real scale. The proposed design has TMD mounted from the center of the structure which has 18% of the structure total mass. The structure should be predesigned and pre-fabricated to decrease the amount of the work for the occupants.

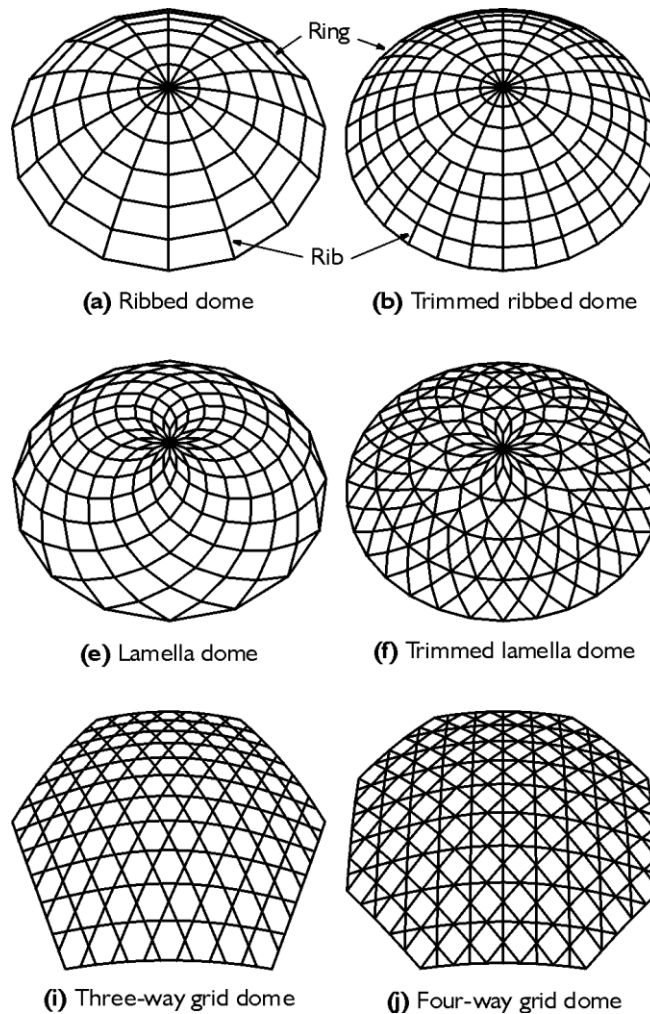


Figure 51: Dome Types

Dome can be built in different ways each has its own geometry. As it is showing in figure 55 the proposed design is in the ribbed dome capacity which is one of the easiest domes to construct. In general, about ribbed dome we can say, it often has a very low weight and is usually used to cover spans of up to 150 meters. Often prefabricated, their component members can either lie on the dome's surface of revolution or be straight lengths with the connecting points or nodes lying upon the surface of revolution. Single-layer structures are called frame or skeleton types and double-layer structures are truss types, which are used for larger spans. When the covering also forms part of the structural system, it is called a

stressed skin type. The best match dome system for this function is the single layer ribbed dome system.

To satisfy the need of the affordable housing; ‘Affordable housing program’ studied and highlighted points presents in this part.

4.1.1 Affordable Housing

What is affordable housing and who need affordable housing?

Based on US community Planning and Development, families who pay more than 30 percent of their income for housing are considered cost burdened and may have difficulty affording necessities such as food, clothing, transportation and medical care.

Based on the US community Planning and Development many people needs to have affordable housing to live and grow their children in a safe house.

In other to overcome the limited budget of the people who live in a high seismic risk area a single story dome shape building presents in this study.

Each building has the minimum function requirement which varies from country to country, area to area. In this research a minimum living place considered to design; based on American Planning Association the following areas are minimum space requirement for each space functions:

- Living Room: 150 Square feet
- Dining Room 80 square feet
- Bedroom 90 Square feet

- Kitchen 60 Square feet
- Library 60 Square feet

To have at least two bedrooms building considering the minimum areas and adding the standard 20-30% hallway and corridor. The program presented as follows

A living room(150 Square feet) + Dining room (80 Square feet) + 2 Bedroom (180 Square feet) + Kitchen (60 Square feet) and two bathrooms (80 square feet).

The total needed area for the single-family building is 550 square feet. The standard corridor and hallway is 30 percent of the total area, therefore; the total area for 2 bedroom building are equal to 715 square feet.

4.1.2 Advantages of the Design

1. Assembling of the proposed structure is straightforward to handle. It can be a good solution to provide long or short term living area for people after/before damage.
2. Long Lasting: Because of the shape and structural response to the environmental forces this structure can last longer than other typical structures.
3. Versatile: This structure should be consists of thin layer of concrete and light steel structure that can be used in many ways / possible to be designed based on the preferences.

4. Maintenance: The structure is designed to withstand harmful elements. So the users have not to spend time and money in maintaining the structure.
5. Portable and easy to assemble: Because of its light weight it is easy to move and assemble elements. All pieces can be modeled and assemble in place easily.
6. Endless Design Possibilities: The design possibilities are almost endless. While it may seem odd at first to try and figure out how to design a round home, the open floor plan allows you to insert or remove walls almost anywhere. A dome home is structurally independent of interior framing, so you don't have to worry about that kitchen wall being "load-bearing".

The monolithic Dome institute [18]

4.1.3 How to Build a Residential Dome

1. Foundation: The construction of a dome starts as a concrete ring foundation, reinforced with steel rebar. Vertical steel bars embedded in the ring later attached to the steel reinforcing of the dome itself. Small domes may use an integrated floor/ring foundation. Otherwise, the floor is poured after completion of the dome.
2. Set the steel structure: This structure needs small diameter bars with wide spacing. Lager domes require larger bars with closer spacing.
3. Air form: An Air form – fabricated to the proper shape and size – is placed on the ring base. Using blower fans, it is inflated and the Air form creates the shape of the structure to be completed.

4. Shotcrete: Shotcrete a spray mix of concrete, it is applied to the exterior and interior surface of the dome. The steel rebar is embedded in the concrete and when about three inches of shotcrete is applied, the Dome is finished.

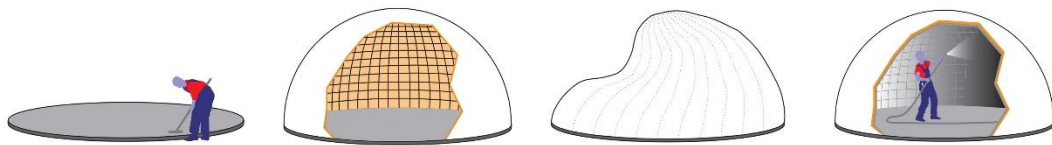


Figure 52: Typical dome Construction Procedure

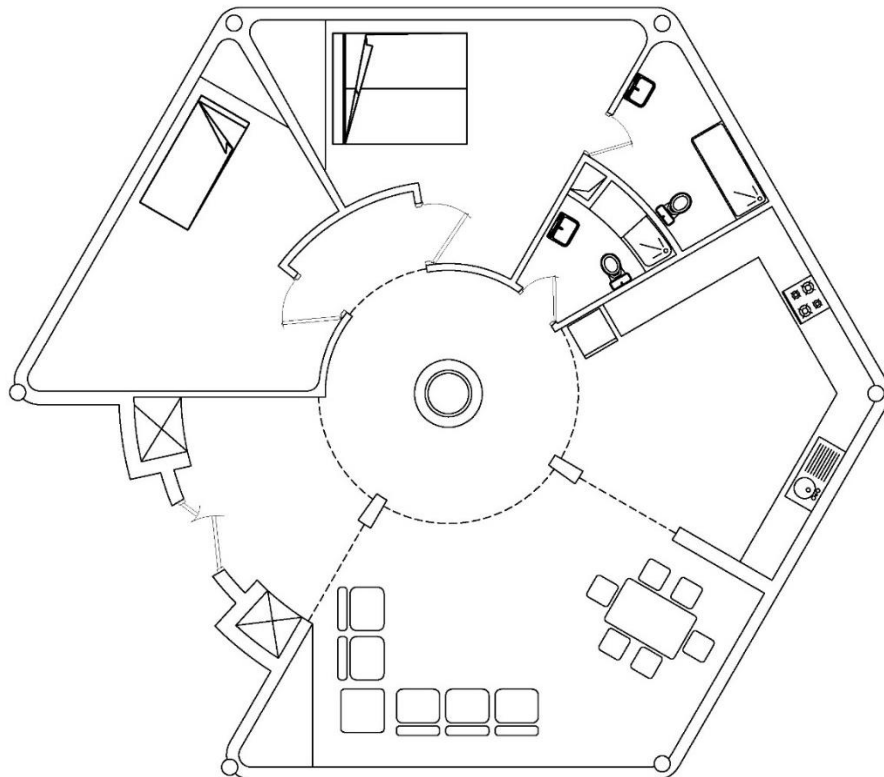


Figure 53: Proposed Architectural proposed design plan view

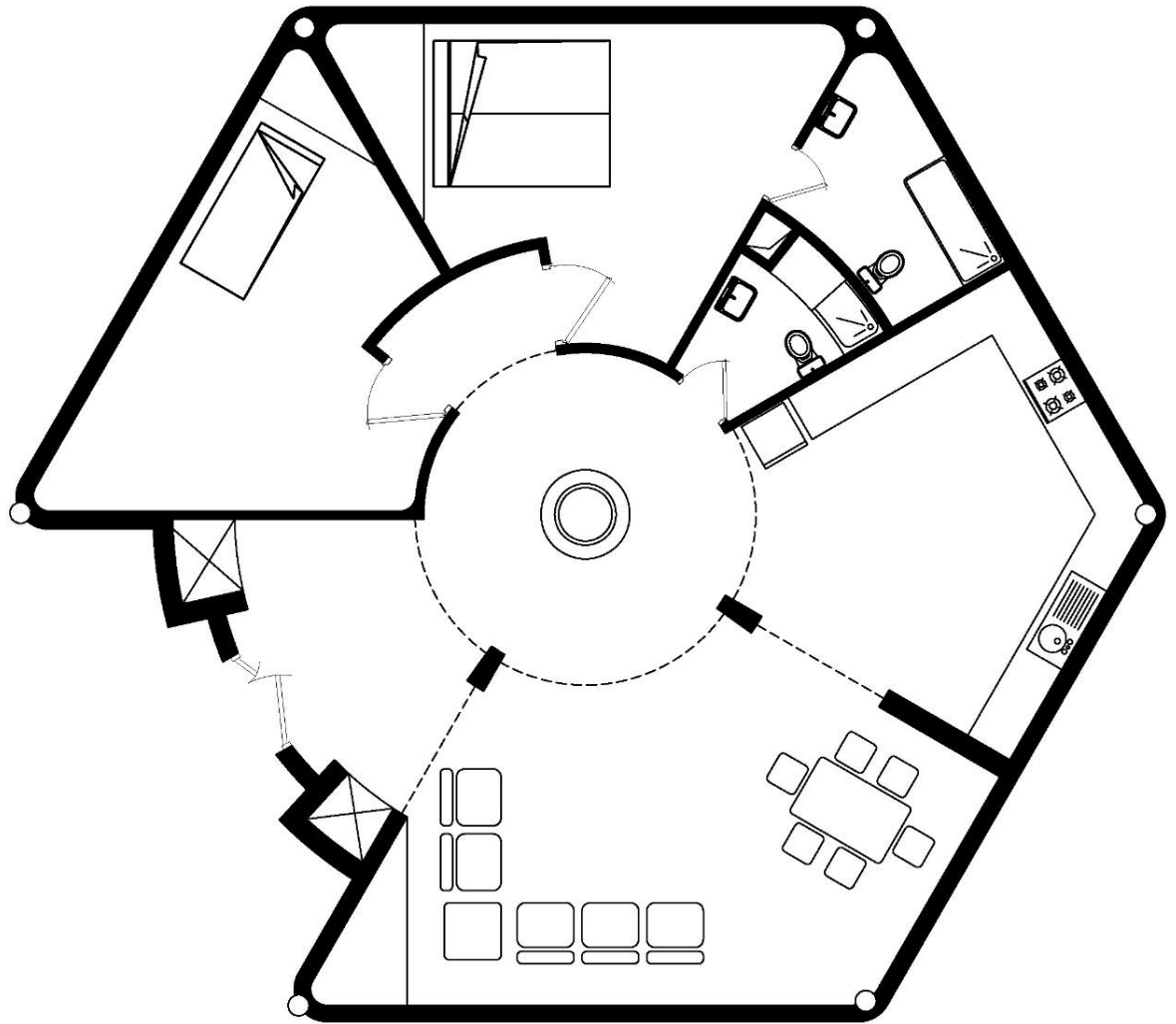


Figure 54: Architectural proposed design plan view

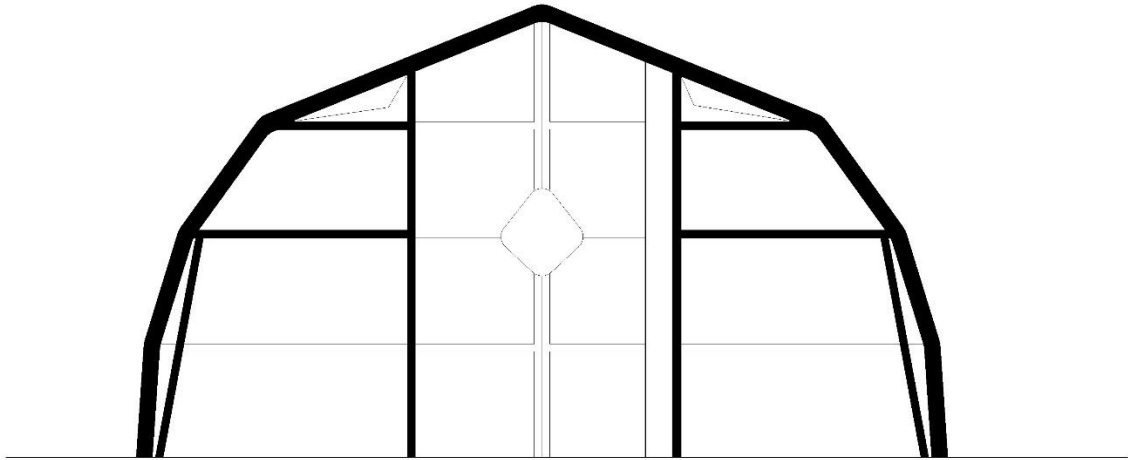


Figure 55: Architectural proposed design section View



Figure 56: Proposed design 3D view

5. CONCLUSION AND FUTURE RESEARCH

5.1 Conclusion

The following conclusions are determined from this investigation:

1. The experimental and theoretical response of the ribbed dome under static loading are in excellent agreement.
2. The predicted dome natural vibration response captures only some key features of the experimental response.
3. The experiment and theoretical response of the dome under both sinusoidal and El Centro earthquake base excitation are in good agreement.
4. Properly designed TMD with efficient design parameters such as tuning, frequency, and mass ratios results in an effective vibration control.
5. The maximum horizontal dome acceleration and apex displacement decreases with the TMD. For example, 18% mass damper decreases the acceleration by 26%.
6. With an increase in the mass ratio for TMD, the apex horizontal displacement decreases up to a particular mass ratio.
7. The maximum acceleration and apex horizontal displacement of the ribbed dome structure is 28% less than the hexagonal structure.

5.2 Future Research:

More detailed research needs to be conducted on the ribbed dome both experimentally and theoretically under dynamic loading conditions. Furthermore, prototype dome need to be analyzed including any attachment needed for dwelling while also satisfying architectural considerations.

References

1. Brownjohn, J.M.W., Carden, E.P., Goddard, C.R., and Oudin, G., 2010. Real-Time Performance Monitoring of Tuned Mass Damper System for a 183 m Reinforced Concrete Chimney, *Journal of Wind Engineering and Industrial Aerodynamics*, 98(3), pp.169-179
2. Building Systems: Design, *Earthquake Engineering and Structural Dynamics*, 39(2), pp.119-139
3. Chang, M.L., Lin, C.C., Ueng, J.M., and Hsieh, K.H., 2010. Experimental Study on Adjustable Tuned Mass Damper to Reduce Floor Vibration Due to Machinery, *Structural Control and Health Monitoring*, 17(5), pp.532-548
4. Chen, G., and Wu, J., 2001. Optimal Placement of Multiple Tuned Mass Dampers for Seismic Structures, *Journal of Structural Engineering*, 127(9), pp.1054-1062
5. Chey, M.H., Chase, J.G., and Mander, J.B., Carr, A.J., 2010. Semi-Active Tuned Mass Damper
6. Gardi, R. (1973) *Indigenous African Architecture*, Van Nostrand Reinhold, London
7. Gerges, R.R., and Vickery, B.J., 2005. Optimum Design of Pendulum-Type Tuned Mass Dampers, *The Structural Design of Tall and Special Buildings*, 14(4), pp.353-368
8. Igusa, T., and Xu, K., 1994. Vibration Control Using Multiple Tuned Mass Dampers, *Journal of Sound and Vibrations*, 175(4), pp.491-503
9. Kirchner, M. (1988) *Technical Evaluation of Dome Type Construction and its Potential as a Housing Form*, Discourse, University of the Witwatersrand.

10. Padmabati Sahoo, 2015. *Experimental and numerical study on Tuned Mass Damper in controlling Vibration of Frame Structure*, Master Thesis, National Institute of Technology.
11. Setareh, M. Ritchey, J.K., Baxter, A.J., and Murray, T.M., 2006. Pendulum Tuned Mass Dampers for Floor Vibration Control, *Journal of Performance of Construction Facilities*, 20(1), pp.64-73
12. Setareh, M. Ritchey, J.K., Murray, T.M., Koo J.H., and Ahmadian, M., 2007. Semi-Active Tune Mass Damper for Floor Vibration Control, *Journal of Structural Engineering*, 133(2), pp.242-250
13. Spencer, B.F., and Sain, M.K., 1997. Controlling Buildings: A New Frontier in Feedback, *Control Systems Magazine*, 17(6), pp.19-35
14. Tedesco, J.W. McDougal W.G. and Ross, C.A., 1999. *Structural Dynamics Theory and Applications*, 1st ed. Addison Wesley Longman Inc.
15. Varoto, P.S., and de Oliveira, L.P.R., 2002. On the Force Drop off Phenomenon in Shaker Testing in Experimental Modal Analysis, *Shock and Vibration*, 9, pp. 165-175
16. Wu, J., and Chen, G. 2000 “Optimization on multiple tuned mass dampers for seismic response reduction” *Proceedings of the American Control Conference*, 0-7803-5519- 523/00.
17. Buckminster Fuller institute <https://www.bfi.org/>
18. The monolithic Dome institute, 2018, <https://www.monolithic.org/domes>
19. Wikipedia, 2013, <http://en.wikipedia.org/wiki/Earthquake>.